



Evaluation of long-term carbon dynamics in afforested drained peatlands: Insights from using the ForSAFE-Peat Model.

Daniel Escobar^{1,2}, Stefano Manzoni¹, Jeimar Tapasco², Salim Belyazid¹

¹ Department of Physical Geography and Bolin Centre for Climate Research, Stockholm University, SE-106 91 Stockholm, Sweden.

² Climate Action, Alliance of Bioversity International and the International Center for Tropical Agriculture (CIAT), Palmira 763537, Colombia.

Correspondence to: Daniel Escobar (daniel.escobar@natgeo.su.se)

Abstract. Afforested drained peatlands have significant implications for greenhouse gas (GHG) budgets, with contrasting views on their effects on climate. This study utilized the dynamic ecosystem model ForSAFE-Peat to simulate biogeochemical dynamics over two full forest rotations (1951-2088) in a nutrient-rich drained peatland afforested with Norway spruce (*Picea abies*) in southwest Sweden. Model simulations aligned well with observed groundwater levels ($R^2 = 0.71$) and soil temperatures ($R^2 \geq 0.78$), and captured seasonal and annual net ecosystem production patterns, although daily variability was not always well represented. Model outputs were analysed under different system boundaries (soil, ecosystem, and ecosystem plus the fate of harvested wood products named ecosystem+HWP) to assess carbon exchanges using the net carbon balance (NCB) and the integrated carbon storage (ICS) metrics. Results indicated negative NCB and ICS across all system boundaries, except for a positive NCB calculated by the end of the simulation at the ecosystem+HWP level. The soil exhibited persistent carbon losses primarily driven by peat decomposition. At the ecosystem level, net carbon losses were reduced as forest growth partially offset soil losses until harvesting. NCB was positive ($1015 \text{ g}_C \text{ m}^{-2}_{\text{soil}}$) at the ecosystem+HWP level due to the slow decay of harvested wood products, but a negative ICS ($-7.0 \times 10^5 \text{ g}_C \text{ yr m}^{-2}_{\text{soil}}$) due to initial carbon losses. This study highlights the importance of system boundary selection and temporal dynamics in assessing the carbon balance of afforested drained peatlands.

1 Introduction

Atmospheric greenhouse gas (GHG) concentrations consistent with the Paris Agreement's long-term temperature goal require ambitious carbon removals during this century (Rogelj et al., 2018). Land management practices can lead to net removals or net exports depending on several controlling factors often hard to quantify and generalize (Crusius, 2020; Guenther et al., 2020; Krause et al., 2020; Seddon et al., 2020). This problem is particularly acute in peatlands, as they are both large carbon stores and are very sensitive to land management.

Forestry on drained peatlands is a widespread land management practice in the northern hemisphere and has significant implications on GHG budgets (Leifeld et al., 2019). This practice is especially common in northern Europe, covering around



5.7, 1.5 and 0.3 million hectares in Finland, Sweden and Estonia respectively (Vasander et al., 2003). Drainage leads to important changes in the carbon dynamics of these systems (Ojanen & Minkkinen, 2019). Lowering the water table promotes forest growth and subsequently carbon accumulation in living biomass in addition to decreasing methane emissions, (Escobar et al., 2022). Nonetheless, higher soil oxygen content associated with lowering the water table promotes decomposition, potentially leading to substantial carbon emissions from peat soils (He et al., 2016). According to Jauhiainen et al. (2023), the soil carbon balance, calculated as the difference between litter inputs and heterotrophic respiration, commonly shows losses for afforested peat soils on northern latitudes, ranging from 21 and 261 $\text{gC m}^{-2} \text{yr}^{-1}$ depending of climate and nutrient status. Restoration of water table levels and wetland vegetation has been proposed as a tool for meeting Paris Agreement targets (Guenther et al., 2020; Tanneberger et al., 2021). Several efforts to restore peatlands are underway. For example, the EU Nature Restoration Law has proposed specific area targets for peatland rewetting (Noebel, 2023). Drained peatlands restored through rewetting exhibit long-lasting differences regarding hydrological and ecological dynamics compared to their pre-drainage status (Kreyling et al., 2021). However, restoration seems capable of reducing soil carbon losses in these systems (Darusman et al., 2023; Escobar et al., 2022).

While restoration holds promise for mitigating climate change, its effectiveness remains a subject of debate due to different views about the effects on climate caused by afforested drained peatlands in northern latitudes (Kasimir et al., 2018; Meyer et al., 2013; Ojanen & Minkkinen, 2020). Whether all types of drained peatlands consistently lose soil carbon is still an open question due to contrasting results from field measurements (Butlers et al., 2024; Hermans et al., 2022; Meyer et al., 2013; Minkkinen et al., 2018). Additionally, disagreement persists regarding the appropriate boundaries for analysing these system, specifically whether carbon accumulated in harvested tree biomass should be included in the carbon budgets of these systems to estimate their impact on climate during a timeframe relevant for climate change mitigation (Kasimir et al., 2018; Ojanen & Minkkinen, 2020).

The importance of the tree biomass components is clear from net ecosystem production (NEP) measurements performed with the eddy covariance technique, which indicate a persistent carbon sink in afforested drained peatlands despite high soil carbon losses (Korkiakoski et al., 2019; Meyer et al., 2013; Tong et al., 2024). It has been recognized that in cases of persistent and large soil carbon losses, compensation through forest uptake is limited because the tree component has a maximum carbon storage capacity lower than the carbon stocks of a typical peat soil. The magnitude and extent of this compensation are likely sensitive to how harvested wood products (HWP) are accounted for. When considering HWP, post harvesting periods are of special relevant suggesting that to understand the trade-off between tree biomass carbon and soil carbon, it is necessary to analyse carbon dynamics over more than one forest rotation. This shows how considering the carbon balance within the soil, ecosystem, or the ecosystem plus the fate of HWP may lead to contrasting results.

Furthermore, due to tree carbon uptake compensation of soil carbon losses, the effects on climate of these systems might be greatly affected by how the forest stand is managed (Tong et al., 2024), which adds uncertainties to the estimated carbon budgets. Indeed, a large area of drained afforested peatlands is likely to undergo conventional forest management in the next few decades. Field-based measurements of carbon balances have shown high temporal variability due to high sensitivity to



65 nutrient status, forest stand characteristics, water table level and temperature (Korkiakoski et al., 2023; Mamkin et al., 2023). Adding to these uncertainties, measurements are usually performed during short periods (Escobar et al., 2022) that do not correspond to the long cycles of conventional forestry.

Utilizing dynamic ecosystem models can provide simulation data about carbon dynamics representative of long periods that can further being analysed under different system boundaries to complement short term measurements (Minkinen et al., 70 2018). Here we introduce the dynamic ecosystem model ForSAFE-Peat and use it for a long-term simulation encompassing two full forest rotations in a heavily studied drained afforested peatland in the southwest of Sweden using mostly parameters previously calibrated. We analysed model outputs to represent different system boundaries and we applied different metrics to quantify carbon exchanges across these boundaries.

In this contribution, we address the following questions:

- 75
- i. Do model outputs resemble field-based observations of soil and vegetation carbon dynamics in a northern drained afforested peatland?
 - ii. Do model outputs indicate different patterns of carbon exchange across different system boundaries for a northern afforested drained peatland?

2 Methods

80 We modified the forest ecosystem model ForSAFE (Wallman et al., 2005; Zanchi, et al., 2021b) to better describe prominent processes in peat soils. We then used the modified model ForSAFE-Peat to simulate biogeochemical dynamics encompassing two full forest rotations of a drained nutrient rich peatland dominated by Norway spruce (*Picea abies*). Site conditions were typical of afforested drained peatlands in southwest Sweden under conventional forestry management practices.

For the first question we compared model outputs to field measurements performed in a heavily monitored site using goodness 85 of fit indicators. For the second question we used model outputs to quantify two carbon exchange metrics under different systems boundaries and we analysed their evolution throughout the period of analysis.

2.1 Model description

ForSAFE-peat simulates daily biogeochemical dynamics building upon the established ForSAFE model (Wallman et al., 2005; Yu et al., 2018; Zanchi, et al., 2021b). This process-based and compartmental model tracks carbon, water and nutrient flows 90 throughout a forest stand ecosystem. A detailed description of the model and its mathematical formulation can be found in the supplementary information section 1; here we only provide a short summary.

The model simulates daily photosynthesis as a function of photosynthetically active radiation regulated by temperature, leaf area, foliar nitrogen content, water availability and atmospheric CO₂ concentration. Photosynthesized carbon and assimilated nutrients are initially allocated within five labile compartments before entering four specific plant compartments (leaves, 95 branches, wood, roots). Carbon and nutrients are either harvested or return to the to the soil through litterfall for further cycling



through decomposition. Woody residues associated to management removals are allocated to an intermediate compartment of deadwood before entering the soil as litter.

Soil is represented by layers defined by the user, and each layer's thickness is allowed to vary during the simulation based on the amount of organic matter it holds while porosity remains constant. Heat is transported vertically according to the heat equation adapted for peat soils. Downward water movement is driven by gravity and modulated by soil hydrological properties, while plants influence water uptake through transpiration. Additionally, specific layers can exchange water horizontally, simulating the impact of drainage ditches on hydrological processes within the peatland.

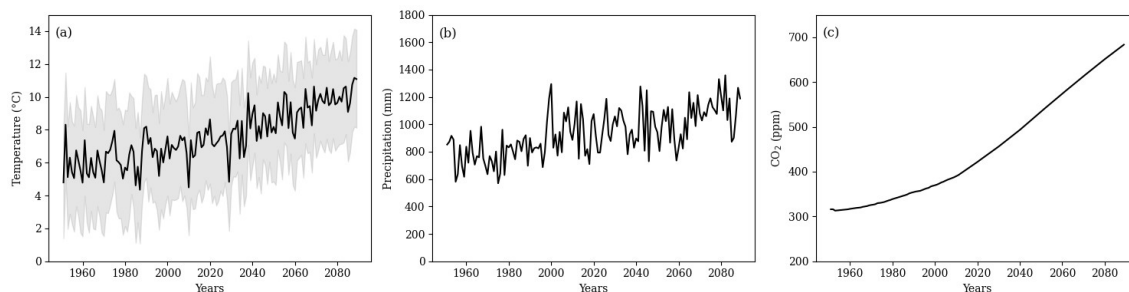
Organic matter within the soil is divided between four solid compartments (easily decomposable compounds, cellulose, lignin and peat) that are decomposed at different rates according to first-order kinetics modified by temperature, moisture, and pH. This process releases dissolved organic compounds (dissolved organic carbon, dissolved organic nitrogen and CH_4) and mineral compounds (CO_2 , NH_4^+ , Mg^+ , K^+ and Ca^+) into the soil solution. Mineral weathering, atmospheric deposition and ion exchange further add, and in the latter may also remove, compounds such as sulphate (SO_4^-), nitrogen ions (NH_4^+ , NO_3^-), base cations (Mg^+ , K^+ , Ca^+), chloride (Cl^-), sodium (Na^+) and aluminium (Al^+) to the soil solution. Soil solution pH is then calculated based on the acid neutralizing capacity of the soil solution. Mass balance equations that account for gas-water partitioning, diffusion, water transport, plant uptake and chemical transformations are used to track the concentration of these elements in the soil.

The model tracks the fate of the carbon within the harvested biomass extracted from the site by allocating it into three compartments (fuel, fibre and hard wood products) whose decay is simulated through first order kinetics and has not integrated feedback to other parts of the model.

2.2 Site and scenario description

We simulated two forest rotations over the period from the beginning of 1951 to the end of 2088 at a drained afforested peatland located at Skogaryd Research Station (<https://meta.fieldsites.se/resources/stations/Skogaryd>) in the southwest of Sweden ($58^\circ 23' \text{N}$, $12^\circ 09' \text{E}$). This site has hemiboreal climate, high nutrient content organic soil, high peat depth, good drainage, and conventional forestry management is adopted. The site, formerly a fen valley, underwent drainage in the late 19th century to facilitate agricultural use before being repurposed for forestry in 1951.

The model used daily mean meteorological data (1951 to 2023) from the Swedish Meteorological and Hydrological Institute (SMHI) Vänersborg ($58^\circ 35' \text{N}$, $12^\circ 35' \text{E}$) and Uddevalla D ($58^\circ 36' \text{N}$, $11^\circ 93' \text{E}$) stations, while future climate data (2023 to 2088) were obtained from projections for forest sites under the CLEO research program (Munthe et al., 2016). Climate projections were downscaled from regional projections based on ECHAM and HADLEY climate model under RCP 6.0 as in (Zanchi, et al., 2021a). Yearly atmospheric deposition was derived from the MATCH model simulation (Engardt & Langner, 2013; Munthe et al., 2016) and scaled based on daily precipitation. Climate data used as an input for the simulations can be seen in Figure 1.



130 **Figure 1. (a) Mean annual temperature (black line) and difference between mean annual maximum temperature and mean annual minimum temperature (grey area). (b) Annual precipitation. (c) Yearly average atmospheric CO₂ concentrations. The time series span both the historical period (from 1951; data from the Swedish Meteorological and Hydrological Institute) and a future period (till 2088; data from model projections; see Section 2.2).**

135 Modelled forest management mimicked historical events in the site: spruce planting in 1951, a 72% tree biomass thinning in 1979, a 10% biomass loss in 2010 due to storm damage and a 96% biomass removal in 2019 due to clear cutting. Harvesting exerts important control over carbon dynamics in these systems. The large thinning event, which removed 72% of the biomass after ~28 years of plantation, represents a non-conventional management practice (Metzler et al., 2024). This intensive management strategy was included in our simulations to accurately reflect the historical management of the real site on which our study is based. The second modelled rotation (2020-2088) followed the biomass removal time patterns of the first rotation.

140 Simulation assumed Norway spruce (*Picea abies*) to be the only vegetation present at the site. Photosynthesis and plant growth parametrizations followed previous studies (Aber et al., 1996, 1997; Zanchi et al., 2021b).

The modelled soil profile, reflecting an average depth of 3 meters as reported by Nyström, (2016), was discretized into 10 layers. Of these, the top nine layers were initially 0.2 m thick, while the bottom layer had a thickness of 1.2 m. At the onset of the simulation, all layers were characterized by the same properties. Bulk density was uniformly set to 0.21 g cm⁻³, informed

145 by on-site observations and corroborated by findings in managed peat (Liu et al., 2020), while organic matter content was assumed to be 87%. Initial soil organic matter (SOM) was allocated entirely to the peat SOM compartment and 50% of it was assumed to be soil organic carbon (SOC). Initial carbon-to-nitrogen (C:N) ratio was set to 21, aligning with the observed average C:N at the site (Eriksson, 2021).

To simulate drainage, at the beginning of the simulation, the layers within a depth of 0.6 m had a lateral outflow of water controlled by their hydraulic conductivities. Because layers can expand or contract within the model structure due to changes

150 in soil organic matter content, the fraction of the vertical soil profile subject to lateral flow changes through time. Ditch network maintenance (DNM) also results in changes in the layers from which lateral outflow is allowed. In order to mimic conventional management after clear-cut, we determined the soil layers within 0.6 m depth in 2022 and allowed horizontal water flow from them.

155 A more detailed description of the scenario parametrization can be found in the supplementary information section 2.



2.3 Simulation representativeness

To evaluate the model's performance in replicating observed variables, we compared model outputs to available observations of abiotic factors controlling carbon dynamics and observations of carbon fluxes. For abiotic factors controlling carbon dynamics we focused on soil temperature and ground water level (GWL) which are regarded as the main regulators of carbon fluxes in drained peatlands (Escobar et al., 2022; Evans et al., 2021; Jauhiainen et al., 2023). Data for net ecosystem exchange
160 representative was available for the entire stand, while data for soil temperature and GWL were available at several distinct locations at the site which were averaged for the numerical comparison with the model estimates. We assessed the coefficient of determination (R^2) and the root mean squared error (RMSE).

For on-site observations, daily groundwater level data spanning six years (2014-2020) were available at four distinct locations.
165 Concurrently, daily soil temperature records covering a 14-year period (2008-2022) were obtained for three depths (0.05, 0.15, and 0.30 meters) at three locations. Measurement methods used at the site are described in Ernfors et al. (2011) and Klemetsson et al. (2010). NEP (i.e. gross primary productivity minus ecosystem respiration) data were obtained from measurements done by eddy covariance (EC) technique for the years. On-site NEP measurements were conducted in 2008 while trees were present on the site, with subsequent data from 2020 and 2021 acquired post-clear-cutting, offering insights
170 into soil respiration in the absence of significant photosynthetic activity. Data processing and acquisition is described in Meyer et al. (2013) and Vestin et al. (2020).

We performed manual calibration of two parameters: the modifier of the bottom layer hydraulic conductivity that controls percolation ($limK_{sat}$) and fraction of wood that respire (RWF). Calibration was made against ground water level observations from two locations from 2008 to 2013 and informed by estimates of biomass on the site from 2008 to 2010 based on tree ring
175 data (He et al., 2016). More information is provided in the supplementary information section 2

2.4 Carbon exchange metrics

While acknowledging the potential significance of N_2O emissions in drained fertile peatlands (Jauhiainen et al., 2023), we focus on carbon dynamics. To evaluate potential effects on climate via carbon exchanges, two metrics related to the carbon balance were selected: the net carbon balance (NCB) and the integrated carbon storage (ICS). The NCB is calculated as:

$$180 \quad NCB(T) = \int_{t_0}^T (Ic(t) - Oc(t)) dt, \quad (1)$$

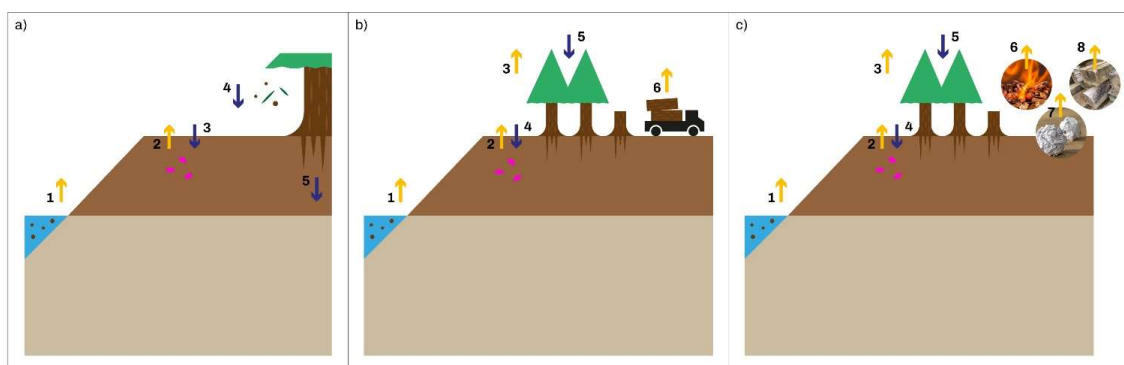
where $NCB(T)$ is expressed in units of mass of carbon per area of reference ($g_C m^{-2}_{soil}$) and is calculated as the carbon gain or loss after integrating the input fluxes of carbon ($Ic(t)$) minus the outputs fluxes of carbon ($Oc(t)$) from the beginning of the period of analysis (t_0) until the end (T). The calculation of the $ICS(T)$ shown in equation (2) can be interpreted as the cumulative carbon storage and is calculated by integrating the $NCB(t)$ throughout the period of the analysis (Sierra, 2024),

$$185 \quad ICS(T) = \int_{t_0}^T NCB(t) dt. \quad (2)$$



Based on equation (2), this metric is expressed as mass of carbon per area multiplied by time ($\text{g}_C \text{ yr m}^{-2}_{\text{soil}}$). The $ICS(T)$ is useful because it accounts for time dynamics of carbon storage, which in turn control the cumulative atmospheric cooling or warming effect a system has (Sierra, 2024; Sierra et al., 2021). When a system exhibits a very dynamic carbon exchange characterized by periods of large net losses and periods of large net gains, the $NCB(t)$ might vary between positive and negative. 190 The interval of time during which accumulated losses exceed accumulated gains can be interpreted as a period of negative effects on climate while the opposite is true for the interval of time during which accumulated gains exceed accumulated losses. This is capture by the $ICS(T)$ by integrating the $NCB(t)$ through a reference time period (T).

We estimated the previously explained metrics for three different system boundaries: the soil, the ecosystem and the ecosystem plus the fate of HWP (ecosystem+HWP). Differences in system boundaries imply different inflows and outflows for equation 195 (1). By examining different system boundaries, we can offer diverse perspectives on the carbon exchanges (and thus the potential effect on climate) of afforested drained peatlands. Additionally, these delineations provide valuable categories for analysing the temporal dynamics of carbon fluxes and their associated controlling factors. Differences in system boundaries are represented and explained in Figure 2.



200 **Figure 2. System boundaries used in the study: a) Soil boundary, b) Ecosystem boundary, and c) Ecosystem + HWP boundary. Yellow arrows represent carbon outflows, and blue arrows represent carbon inflows. Soil boundary a): carbon leaching (arrow 1), soil-atmosphere carbon exchange (arrow 2 and 3), litterfall (arrow 4) and belowground autotrophic respiration (arrow 5). Ecosystem boundary b): carbon leaching (arrow 1), above-ground autotrophic respiration (arrow 3), soil-atmosphere carbon exchange (arrow 2 and 4), photosynthesis (arrow 5), tree harvesting (arrow 6). Ecosystem + HWP boundary c): carbon leaching (arrow 1), above-ground autotrophic respiration (arrow 3), soil-atmosphere carbon exchange (arrow 2 and 4), photosynthesis (arrow 5), outflows from the decay of HWPs (arrows 6, 7 and 8).** 205

Leached carbon might be in the form of dissolved methane (CH_4), carbon dioxide (CO_2) and dissolved organic carbon (DOC). Furthermore, we considered the gas exchange of CO_2 and CH_4 between the atmosphere at the soil which can be outflow or inflow based on the concentration gradient. We did not account for chemical transformations of leached carbon that can happen 210 in ditches and streams. For all these system boundaries, outputs are indicated by negative fluxes and inputs by positive fluxes.



3 Results

3.1 Simulation representativeness

The model captured daily observations of groundwater table and soil temperature relatively well, but less so for daily NEP. However, simulated annual and seasonal NEP are closely comparable to the observations.

215 3.1.1 Abiotic factors

Observed groundwater levels from 2014 to 2021 had a mean of -0.45 m and a standard deviation of 0.17 m. Summer lower values before clear cutting ranged between -0.6 and -0.9 m. The high summer groundwater levels observed after 2020 are attributed to the final felling of 2019, which decreased transpiration thereby increasing groundwater levels. While considerable variance exists among observations at different locations, the simulations generally fell within this range (Figure 3a). The R^2 between average observed and simulated water table depths was 0.71 and the RMSE -0.09 m (b). The model reliably reproduced observed groundwater level but with a clear although relatively small underestimation particularly manifesting during winters. The model simulated lower groundwater levels during winter compared to the average among the four locations. However, this lower water table is not expected to significantly impact soil CO_2 emissions, as decomposition is impeded by low temperatures. Conversely, the model showed slightly higher groundwater levels during the driest summers, which is primarily influenced by evapotranspiration.

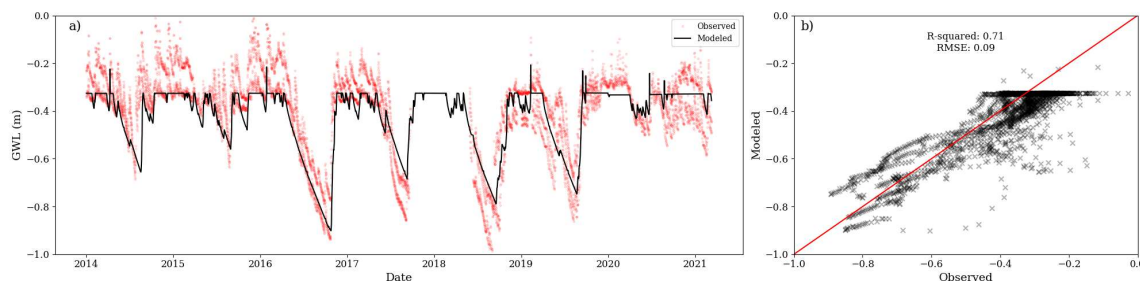
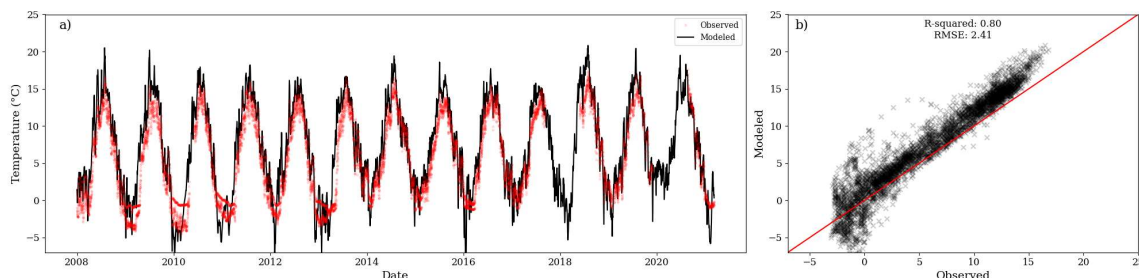


Figure 3.(a) Modelled height of GWL (black line) and observations (red dots), negative values mean distance to the surface. b) Correlation between the average of observed values and modelled values.

230

Daily temperature from 2008 to 2021 exhibited low variability between locations. Observed mean annual soil temperature at 0.05 m depth was 5.5 °C and the standard deviation was 5.4 °C. Simulated soil temperature in the first layer correlated strongly with average observed temperature at 0.05 m among the three measurement locations (R^2 of 0.80, RSME of 2.41 °C) as shown in Figure 4b. Similar comparisons of soil temperature at depths of 0.15 and 0.30 m are given in the appendix A, with R^2 values of 0.78. Simulated soil temperature showed slight but consistent overestimations over observations during spring and summer which could lead to overestimation of the decomposition temperature modifier function (Figure 4a).

235



240 **Figure 4.**(a) Modelled temperature for the first layer (black line) and observations at 0.05m depth (red dots). (b) Correlation between observed and modelled values. During the period of comparison, the centroid of the first layer was between 0.089 m and 0.094m.

3.1.2 Carbon fluxes

NEP measurements revealed the site acting as a net sink of CO₂ in 2008 while still forested, transitioning to a CO₂ source in 2020 and 2021 after clear-cutting. While during 2008 the mean NEP was 0.55 g_C m⁻²_{soil} d⁻¹, during 2020 and 2021 the mean
 245 NEP was -1.08 and -0.59 g_C m⁻²_{soil} d⁻¹ respectively. Despite reproducing soil temperature and GWL reasonably well on a daily basis, the model failed to capture daily changes in NEP (Figure 5a). However, when aggregated to seasonal values the model performed adequately. For fluxes aggregated over warm months (May, June, July, August, September and October) and cold months (November, December, January, February, March, and April) the model achieved R² = 0.88 and RMSE = 55 g_C m⁻²_{soil} half-yr⁻¹ (Figure 5b). The model captured annual NEP fluxes satisfactorily. For 2008, 2020, and 2021 observations were 204,
 250 -396, and -216 g_C m⁻²_{soil} yr⁻¹ respectively, while modelled values were 152, -446, and -383 g_C m⁻²_{soil} yr⁻¹ respectively.

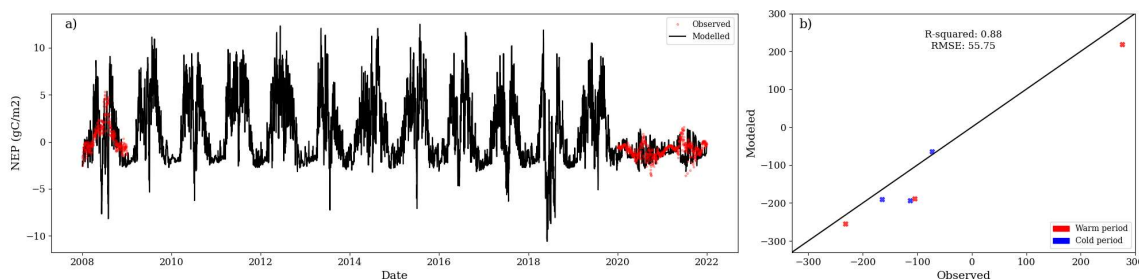


Figure 5. (a) Modelled NEP (black line) and observations (red dots). (b) Correlation between observed values and modelled values. Values for correlation correspond to aggregation of fluxes into warm and cold periods of the year.

255



3.2 Carbon exchange dynamics across system boundaries.

The simulated NCB and ICS are negative under all system boundary assumptions, with the exception of the NBC at the ecosystem+HWP scale. Both metrics were strongly and similarly sensitive to system boundaries (Table 1). The expansion of the system boundaries had a positive effect on both the NCB and ICS, with the soil acting as a stronger source than the ecosystem, which is in turn a stronger source than the ecosystem+HWP. Under the ecosystem+HWP boundaries, despite accumulating more carbon than it loses by the simulation end, the ICS remains negative, indicating a potential persistent negative effect on climate over the same period.

Table 1. Metrics (NCB and ICS) for the soil, ecosystem and ecosystem+HWP as system boundaries at the end of two forest rotation.

System boundaries	NCB ($\text{g}_C \text{ m}^{-2}_{\text{soil}}$)	ICS ($\text{g}_C \text{ yr m}^{-2}_{\text{soil}}$)
Soil	-46173	-3.3×10^6
Ecosystem	-37466	-1.6×10^6
Ecosystem+HWP	1015	-7.0×10^5

265

The main carbon dynamics during the simulation are depicted in Figure 6. Within the soil, the peat compartment decreased with time. Peat losses were not compensated by soils compartments associated with litter and biomass residues despite significant increments in those compartments during the second rotation. The plant carbon compartments were modulated by the cycle of forest management and environmental conditions, which increased plant carbon during the second rotation. HWP carbon compartments significantly increased after 2019's clear cut.

270

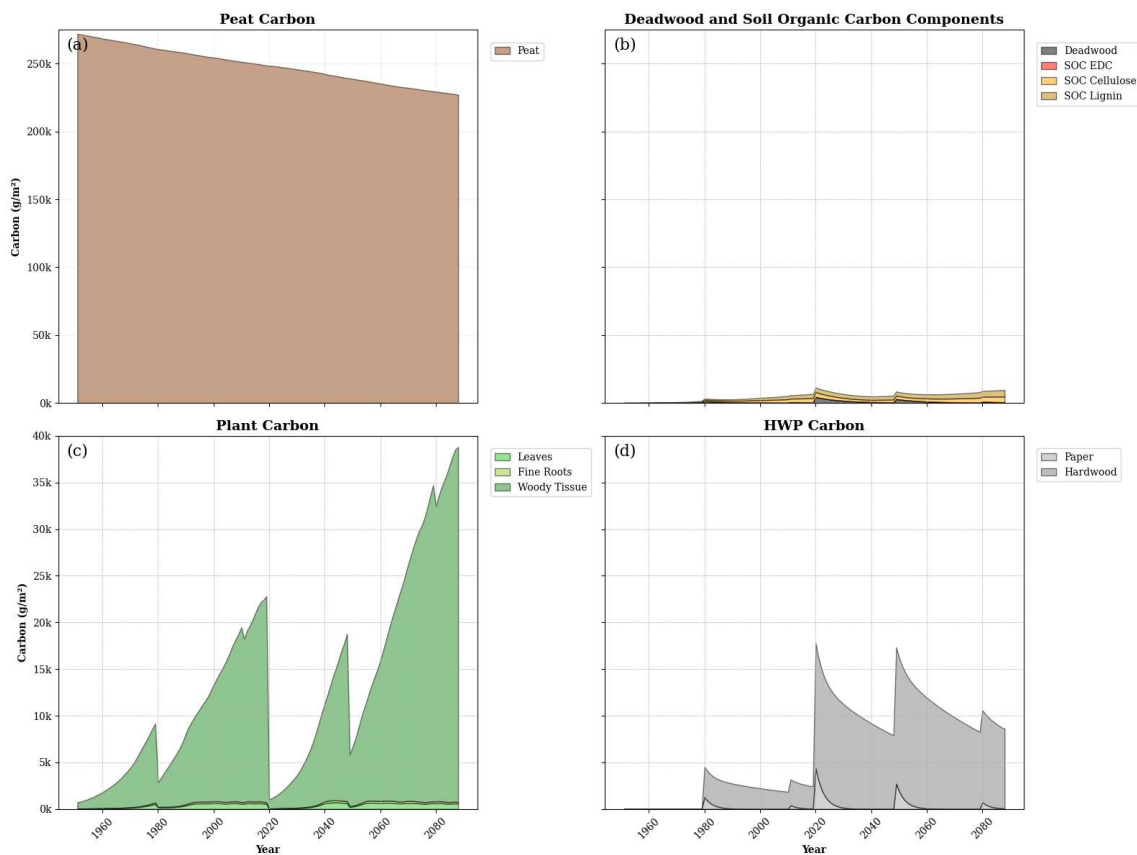


Figure 6. Temporal evolution of main carbon compartments during the simulation. Note the difference in scale of the y axis between the upper plots row plots and the lower plots row.

275

3.2.1 Soil carbon dynamics

At the end of the simulation, for the soil system alone, the NCB was $-46173 \text{ g}_C \text{ m}^{-2} \text{ soil}$ while the ICS was $-3.3 \times 10^6 \text{ g}_C \text{ yr m}^{-2} \text{ soil}$. The NCB declined consistently over time, with the exception of transient recovery events associated with inputs of harvest residues (b). This reflects the persistent net loss of carbon despite the continuous inputs of litter to the soil (a). The ICS declined exponentially with time, as it accounts for the compounding effects of the emitted carbon residing in the atmosphere (Figure 7c).

280

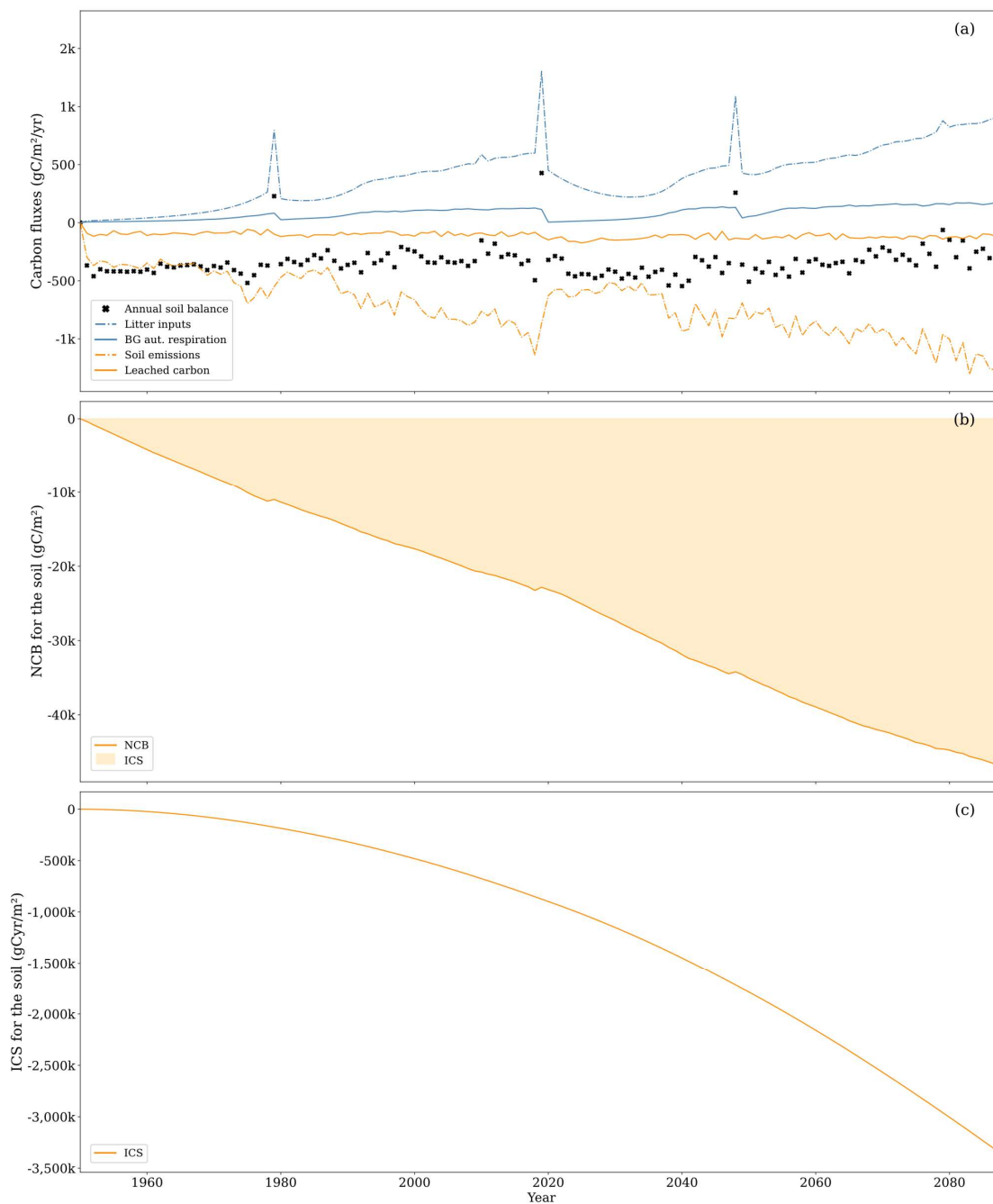
The average annual carbon balance within the soil amounted to $-334 \text{ g}_C \text{ m}^{-2} \text{ soil yr}^{-1}$, showing no significant differences between the first rotation ($-330 \text{ g}_C \text{ m}^{-2} \text{ soil yr}^{-1}$ on average) and the second rotation ($-338 \text{ g}_C \text{ m}^{-2} \text{ soil yr}^{-1}$ on average). Key inflows included



litterfall and carbon transfers from deadwood, primarily dead stumps left after harvest. The most significant outflow was
285 through soil CO₂ emissions, whereas leached DOC and CO₂ contributed only 10% and 4% of total outflows respectively. The
annual balance was lowest at the onset of the forest rotation, due to low litter input and significant soil CO₂ emissions from
peat decomposition. For example, the annual balance was -413 g_C m⁻²_{soil} yr⁻¹ during the first five years of the first forest rotation
while it was -309 g_C m⁻²_{soil} yr⁻¹ during the last 8 years of the first forest rotation. As the tree stand matured, the balance became
less negative, occasionally turning positive during years with large litterfall inputs (e.g., 1283 g_C m⁻²_{soil} yr⁻¹ as a result of the
290 clear cut at the end of 2019).

Litter inputs (not considering years of harvest) notably increased during the second rotation (395 g_C m⁻²_{soil} yr⁻¹) compared to
the first rotation (238 g_C m⁻²_{soil} yr⁻¹), attributed to significantly higher tree biomass. Litterfall is heavily influenced by the size
of the plant compartment they originate from. Leaf litter and root turnover were less influential as the forest matured, with
woody litter assuming more importance. Deadwood carbon transfer became particularly significant post-clear-cut in 2019,
295 compensating for low litter from small trees at the outset of the second rotation, becoming the primary input for the first 14
years of this rotation. During the first rotation deadwood transfer from dead stumps left after removals from management were
on average 36 g_C m⁻²_{soil} yr⁻¹ while during the second rotation were significantly higher amounting to 107 g_C m⁻²_{soil} yr⁻¹.

CO₂ emissions from the soil were also higher during the second rotation (-856 g_C m⁻²_{soil} yr⁻¹) compared to the first rotation (-
586 g_C m⁻²_{soil} yr⁻¹), partly due to increased carbon inputs from litter and deadwood, resulting in higher CO₂ emissions from the
300 EDC, cellulose and lignin SOC compartments. Nonetheless, emissions from peat decomposition remained the primary source
of CO₂ throughout the simulation, with similar magnitudes between rotations. The decreasing availability of peat in the first
three soil layers over time was offset by higher decomposition rates driven partially by increasing soil temperature. During the
first rotation the average peat decomposition rate constant for the first, second and third soil layer were 0.012, 0.010 and
0.006yr⁻¹ respectively, for the second rotation the rate constants were 0.014, 0.012 and 0.011yr⁻¹. Additionally, peat available
305 for aerobic decomposition from layers affected by ditch maintenance after the 2022 further supported persistent and high peat
decomposition rates.





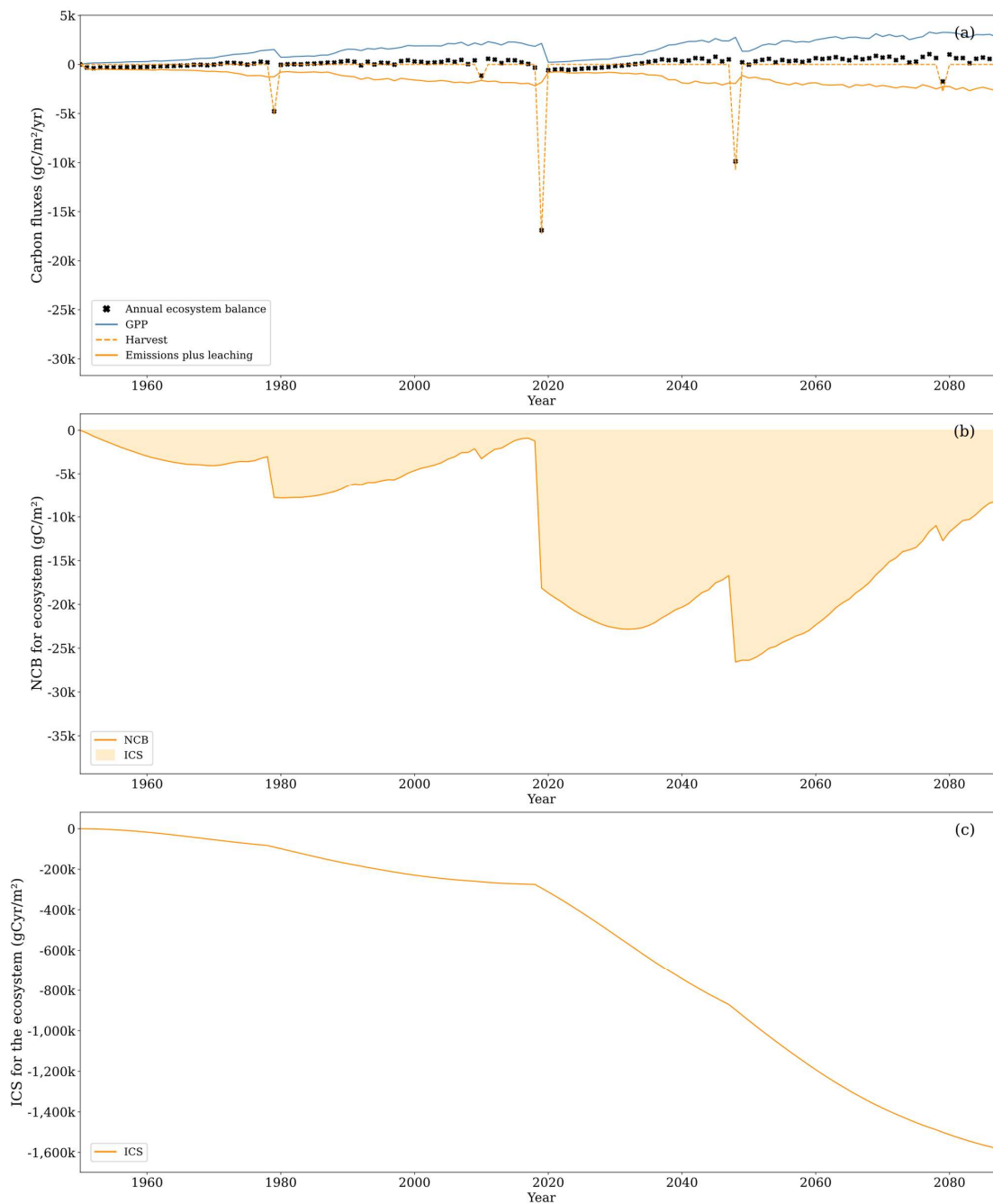
310 **Figure 7. (a) Litterfall from trees and dead wood transfers to soil (dashed blue line), autotrophic below ground respiration (solid blue line), CO₂ soil emissions (orange dashed line) and leached carbon composed of CO₂ and DOC (orange solid line). Note that, for this boundary, autotrophic below ground respiration is an inflow of carbon to the soil. This increases soil CO₂ concentrations which in turn drive CO₂ soil emissions. Uptake of CH₄ and leached CH₄ were excluded from the graph as they comprised less than 1% of the total carbon flux. (b) NCB (solid line) during the period of analysis and the ICS (shaded area). (c) ICS (solid line).**

3.2.2 Ecosystem carbon dynamics

315 Focusing solely on the soil boundaries overlooks the primary mechanism through which afforested drained peatlands accumulate carbon, which is the living tissue of trees. Therefore, analyzing carbon dynamics within the ecosystem boundaries becomes essential. Under these boundaries, both metrics reveal a system with less negative carbon balance compared to the system defined by the soil boundaries, but still negative throughout the analysis period (Figure 8). By the end of the period of analysis, NCB was $-37466 \text{ g}_C \text{ m}^{-2}_{\text{soil}}$, while ICS was $-1.6 \times 10^6 \text{ g}_C \text{ yr m}^{-2}_{\text{soil}}$. Both metrics worsened from the end of the first
320 rotation to the end of the second rotation.

Under these boundaries, the average annual carbon balance amounted to $-271 \text{ g}_C \text{ m}^{-2}_{\text{soil yr}^{-1}}$. If harvest years are not accounted for the balance turns positive ($198 \text{ g}_C \text{ m}^{-2}_{\text{soil yr}^{-1}}$). Inflows are fundamentally exclusive from the spruce stand GPP (i.e. the site was a small sink of CH₄), while the most significant outflows included CO₂ emissions from the soil, aboveground autotrophic respiration, and biomass harvesting, making up 37%, 32%, and 25% of total outflow, respectively. The temporal dynamics of
325 flows explain the results for NCB and ICS. Early carbon losses during the rotation were gradually offset by the rapid growth of GPP. The tree biomass accumulates a fraction of the GPP, offsetting partially the accumulated soil losses until harvest removes tree biomass, sinking the accumulated balance again. The metrics became more negative during the second rotation because sustained soil carbon losses were compounded with the soil carbon losses of the first rotation that were not compensated at the end of the first rotation.

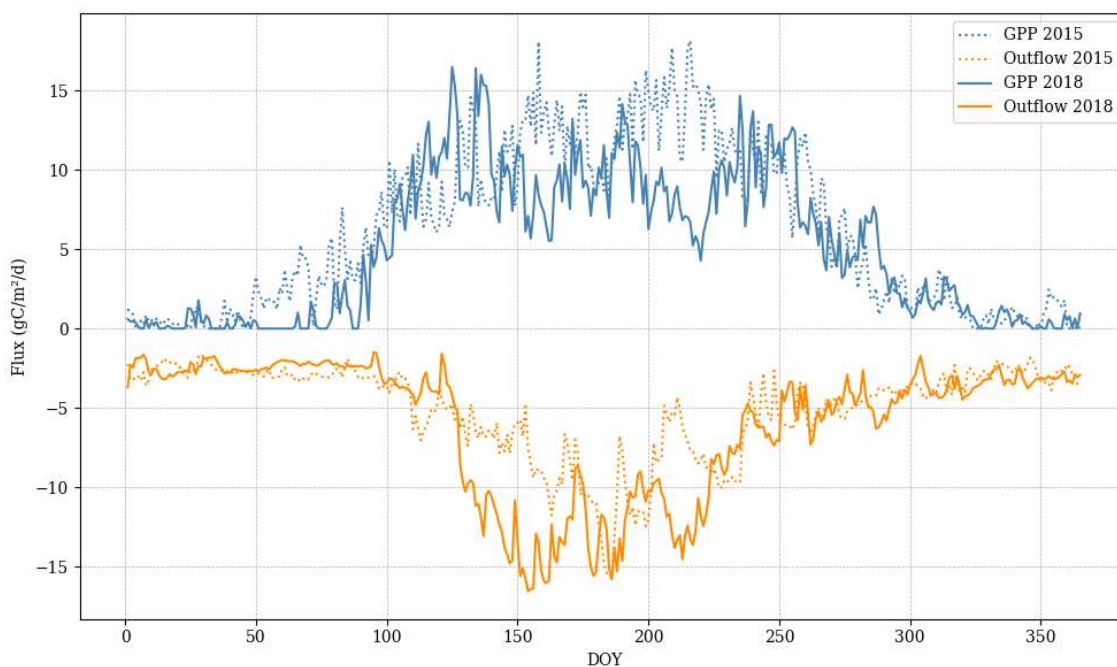
330 During the second rotation, GPP notably increased to $2102 \text{ g}_C \text{ m}^{-2}_{\text{soil yr}^{-1}}$, compared to $1225 \text{ g}_C \text{ m}^{-2}_{\text{soil yr}^{-1}}$ during the first rotation. The increased photosynthetic rates are primarily attributed to the positive effect of higher atmospheric CO₂ concentration and higher temperature embedded in the model formulation. This sets off a reinforcing loop where higher potential photosynthesis leads to increased biomass growth resulting in a high leaf area index (LAI) that further boosts photosynthesis. This can be counter balanced by several processes, such as self-shading, foliar nitrogen dilution and water
335 limitation. While in both rotations maximum LAI values were similar being around $6.5 \text{ m}^2_{\text{leaf m}^{-2}_{\text{soil}}}$, the average LAI during the first rotation ($3.3 \text{ m}^2_{\text{leaf m}^{-2}_{\text{soil}}}$) was significantly lower than the average value for the second rotation ($4.5 \text{ m}^2_{\text{leaf m}^{-2}_{\text{soil}}}$), indicating trees achieving maximum canopy faster in the second rotation. Average foliar nitrogen content expressed as percentage of leaf dry weight remained similar between rotations (1.46%). This was supported by consistently high nitrogen mineralization, during the first rotation average yearly nitrogen mineralization was $6.54 \text{ g}_N \text{ m}^{-2}_{\text{soil yr}^{-1}}$ while during the second rotation average
340 yearly nitrogen mineralization was $8.56 \text{ g}_N \text{ m}^{-2}_{\text{soil yr}^{-1}}$. Similarly, water limitation was not important in neither of the rotations, the ratio between actual plant water uptake and potential plant water uptake was 0.97 in both rotations.





345 **Figure 8. (a) Gross primary productivity (solid blue line), aboveground respiration, soil CO₂ emissions) and leached carbon composed of CO₂ and DOC (orange solid line), carbon outputs due to harvesting (orange dashed line). Uptake of CH₄ and leached CH₄ were excluded from the graph as they comprised less than 1% of the total carbon flux. (b) NCB (solid line) and ICS (shaded area). (c) ICS (solid line)**

In years without harvesting or extreme climatic conditions, GPP typically remains sufficiently high to offset ecosystem carbon loses, except during initial years of a rotation when LAI is less than 0.5 m²_{leaf} m⁻²_{soil}. Extreme climatic conditions lead to a
 350 negative annual carbon balance, even in mature stands with high photosynthetic capacity (i.e. LAI > 6 m²_{leaf} m⁻²_{soil}). For instance, in 2018, when precipitation was 25% below the average for 2005-2019, the annual ecosystem balance was -380 g_C m⁻²_{soil} yr⁻¹. Conversely, in 2015, with precipitation 8% above the average, the balance was 341 g_C m⁻²_{soil} yr⁻¹. During 2018, GPP was 0.81 of 2015 GPP due to water limitations during the summer. Aboveground respiration remained high in 2018 despite lower growth due to plant maintenance respiration, suggesting that the negative effect on carbon fluxes of dry years
 355 can actually be amplified by the size of the forest stand. Soil emissions in 2018 were 1.3 times of those of 2015, suggesting that water limitation to decomposition in the upper soil layers is overridden by aerobic decomposition in deeper peat layers that remained moist (Figure 9).



360 **Figure 9. Comparison between main ecosystem fluxes between a dry year (2018) and a normal year (2015). Outflow is comprised of soil CO₂ emissions, carbon leached and aboveground respiration.**



During most of the years, carbon accumulation in the plant compartment is more than the carbon lost by the soil compartments. Therefore, overlooking removals of plant carbon by harvesting—amounting to 27% of the total carbon outflow from the ecosystem—could falsely suggest a carbon sink within the system. Across the two rotations, harvesting contributed to an
365 outflow of $-67272 \text{ g}_C \text{ m}^{-2} \text{ soil}$ out of the $229598 \text{ g}_C \text{ m}^{-2} \text{ soil}$ photosynthesized by the plants.

3.2.3 Ecosystem+HWP carbon dynamics

Under the ecosystem boundaries, carbon associated with harvested biomass is treated as an outflow, as if harvested carbon were in the form of CO_2 or DOC. However, harvested wood does not undergo rapid conversion to CO_2 . Consequently, the ideal boundaries for assessing effects on climate are those in which all outflows from the system ultimately leave as CO_2 .

370 Within the ecosystem+HWP system boundaries, harvested wood fate is tracked until its degradation into CO_2 , providing a comprehensive view on potential effects on climate. By the end of the period of analysis, the NCB turned positive at $1015 \text{ g}_C \text{ m}^{-2} \text{ soil}$, while ICS was large and negative at $-7.0 \times 10^5 \text{ g}_C \text{ yr m}^{-2} \text{ soil}$ (Figure 10). Both metrics declined by the end of the second rotation compared to the end of the first, when NCB was $1476 \text{ g}_C \text{ m}^{-2} \text{ soil}$ and ICS was $-1.6 \times 10^5 \text{ g}_C \text{ yr m}^{-2} \text{ soil}$. This trend can be
375 attributed to the compensation of early soil carbon losses by forest growth that is not completely cancelled by harvesting due to slow decay of some harvested carbon. The capacity of wood products to hold carbon for some time resulted in a positive carbon balance by the end of each rotation. However, the ICS displays a negative trend because the initial losses are substantial and later compensation is neither sufficient nor sustained long enough to counterbalance the extent and duration of the negative carbon balance under these system boundaries.

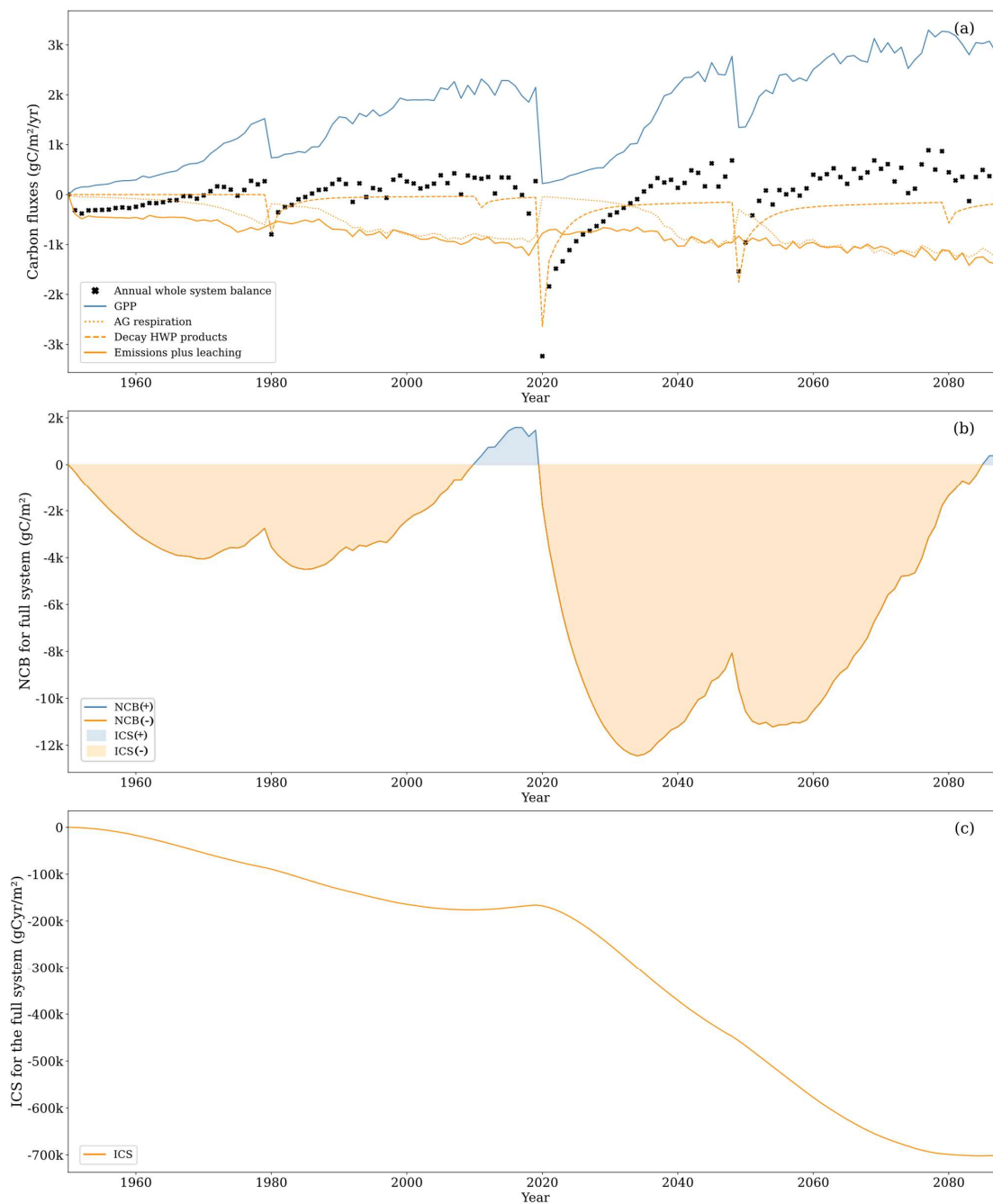
In the ecosystem+HWP system boundaries, the primary inflow of carbon was GPP, with negligible soil uptake of CH_4 . The
380 most significant outflows were, in order of importance, soil carbon emissions, above-ground respiration, degradation of harvested wood and soil carbon leaching. Above-ground respiration increased during the rotation because it is largely controlled by plant biomass. On average, above-ground respiration accounted for 36% of GPP, with lower values during the initial years of the simulation (around 29% in the first five years) and higher values as above-ground woody biomass became a higher proportion of the plant biomass (around 42% in the last five years of the first rotation). Notably, changes between rotations
385 were minimal.

Throughout each rotation, soil carbon losses decreased by higher inputs of fresh litter from larger plant biomass. In the initial 10-year period, soil losses represented 220% of GPP, gradually decreasing to 50% in the final 5 years of the first rotation. Similar values were obtained for the subsequent rotation. Harvested wood degradation peaks during the year of harvest, directly proportional to the harvested biomass, with temporal dynamics independent of GPP fluctuations. During the second rotation,
390 the total carbon lost from harvested wood degradation was 5% of total GPP. Carbon outflows from harvested wood increased during the second rotation because carbon decay from the harvested wood during the 2019 clear-cut event were significant for the first 20 years of the second rotation.

Clear cutting changed the carbon balance drastically at the end of the first rotation. From 1986 until 2019 the annual rate of change of the NCB is positive ($175 \text{ g}_C \text{ m}^{-2} \text{ soil yr}^{-1}$), which led to a positive NCB since year 2010 until 2019. During that period,



395 the ICS negative trend slowed down. The effect of clear-cut in 2019 quickly reduced the NCB, which experienced a strong negative rate of change during the first 10 years of the second forest rotation ($-1263 \text{ gC m}^{-2}_{\text{soil}} \text{ yr}^{-1}$). The NCB was projected to become slightly positive only until 2085. The year after the clear cut, GPP would be reduced by 90% compared to the previous year, soil emissions would remained high while decay of HWP would be 10 times larger than the GPP.





400 **Figure 10.** (a) Gross primary productivity (solid blue line), aboveground respiration (orange dotted line), soil carbon losses comprising soil CO₂ emissions and leached carbon composed of CO₂ and DOC (orange solid line) and CO₂ from products made out of wood harvesting (orange dashed line). Uptake of CH₄ and leached CH₄ were excluded from the graph as they comprised less than 1% of the total carbon flux. (b) NCB (solid line) and ICS (shaded area). (c) ICS (solid line).

4 Discussion

405 4.1 On the representativeness of simulated carbon dynamics and the abiotic context

Site conditions can drastically change the magnitude of carbon fluxes in northern afforested drained peatlands; therefore, soil emission factors for this land category are classified according to climatic and nutrient categories (Wilson et al., 2016). Average modelled soil temperature of 7.0°C for the period of 1990 to 2020 is similar to those found in cool temperate or hemiboreal sites in the south of Sweden or Estonia (Minkkinen et al., 2007; Ranniku et al., 2024). Simulated water table is representative of a well-drained site with functional ditches. During the first rotation, the average GWL was -0.43 m—similar to other drained afforested peatlands (Leppä et al., 2020; Maljanen et al., 2012; Menberu et al., 2016). Spatial variability of GWL within one site can be high, as illustrated by differences across locations within the site. This is often associated with the effect of distance from the ditch network (Laudon & Maher Hasselquist, 2023). Reported mean annual GWL values are often around -0.3 m and -0.5 m for distances from the ditch of 5 m and 15 m respectively (Haapalehto et al., 2014). Groundwater level tends to increase during the rotation in afforested drained peatlands due the combined effects of subsidence and ditch degradation on drainage (He et al., 2016). In our model formulation this behaviour arises because decomposition leads to shrinkage in layers of peat where there is water lateral flow. In our simulations, GWL had slightly lower values during the first 34 years of the rotation (-0.45 m) than during the last 35 years (-0.42 m). Simulated site nutrient conditions—soil organic matter C:N ratio of 21—are similar to other very nutrient rich drained peatlands. Under these conditions sites are often classified as *Herb-rich* type (Ojanen et al., 2010) or eutropic (Minkkinen et al., 2020).

Given the site characteristics, it is understandable why our estimates of litterfall minus soil CO₂ emissions during the first rotation (-341 g_C m⁻² yr⁻¹) are similar to those found in afforested peatlands previously used for agriculture at the same latitude (-256 g_C m⁻² yr⁻¹) by a meta-analysis of field-based observations (Jauhiainen et al., 2023). Despite our values being more negative, they are still well within the variability reported (Jauhiainen et al., 2023; Jovani-Sancho et al., 2021; Lazdiņš et al., 2024). Comparable observations for soil CO₂ emissions are mostly limited to dark chamber measurement that did not remove litter and that include belowground autotrophic respiration. As an example, Arnold et al., (2005) estimated soil CO₂ emissions at -388 g_C m⁻² yr⁻¹ for an afforested drained peatland with a 50-year old Norway spruce stand. In contrast, our estimation for the first rotation, when our spruce stand was between 45 and 55 years old, was -716 g_C m⁻² yr⁻¹. While these sites shared some similarities, such as the grown tree species, the site described by Arnold et al., (2005) had lower nitrogen availability (C:N ratio of 28), lower carbon content (bulk density of 0.17 g cm⁻³), and a higher water table (-0.27 m). Overall, the literature exhibits significant variability, and our estimations tend to fall on the higher end of this range. For instance, Ball et al. (2007)



estimated soil emissions at $-610 \text{ gC m}^{-2} \text{ yr}^{-1}$ for a 30-year-old Spruce stand, compared to our estimation of $-651 \text{ gC m}^{-2} \text{ yr}^{-1}$ for a 29-year-old stand in 1978, before thinning in 1979.

DOC leaching is often assumed to be a less important component of the soil carbon outflux than soil CO_2 emissions and is not often reported. Wilson et al. (2016) estimated $-30 \text{ gC m}^{-2} \text{ yr}^{-1}$ for temperate afforested drained peatlands, but lack of data did not allow to separate fluxes by nutrient status. We calculated an average of $-72 \text{ gC m}^{-2} \text{ yr}^{-1}$ during the first rotation. However, our ratio of soil CO_2 emissions to DOC exports of 0.14 was similar to the 0.12 of Wilson et al. (2016). Interestingly, the ratio between leached DOC and GPP in our study (0.05) was around the average ratio of 0.04 (range: 0.002 to 0.08) estimated for Swedish watersheds by Manzoni et al. (2018). Notably, these ratios in our study were much higher during the first years of rotation due to the effect of drainage and absence of significant photosynthetic activity, highlighting the impacts of processes such as clear cuts (Gundale et al., 2024).

Estimations of annual litter inputs in 35-year-old spruce stands under a long term soil warming fertilization study in northern Sweden by Leppälampi-Kujansuu et al. (2014) align closely with our simulated values ($264 \text{ gC m}^{-2} \text{ yr}^{-1}$) for our stand prior to the 1979 thinning, when it was 28 years old. Correspondingly, similar litter input values ($212\text{-}356 \text{ gC m}^{-2} \text{ yr}^{-1}$) have been reported for young Norway spruce stands (~30 years old) in nutrient-rich conditions slightly north of our site (Blaško et al., 2022). Furthermore, literature findings regarding Norway spruce stands in Finland (Hilli, 2013), Estonia (Uri et al., 2017), and Latvia (Bārdule et al., 2021) demonstrate comparability with our estimates. However, our study may have overestimated litter inputs from woody tissue and foliage, as indicated by measurements conducted by Hilli (2013).

The magnitude of litterfall is closely tied to plant biomass, which increases with GPP fluxes (Ojanen et al., 2014). GPP observations are often derived from net ecosystem production (NEP) measurements using partitioning assumptions. For instance, Mamkin et al. (2023) reported a five-year average GPP of $1494 \text{ gC m}^{-2} \text{ yr}^{-1}$ for old Norway spruce on peat in Russia with an average LAI of $3.5 \text{ m}^2_{\text{leaf}} \text{ m}^{-2}_{\text{soil}}$, comparable to our estimation of $1432 \text{ gC m}^{-2} \text{ yr}^{-1}$ for LAI values ranging between 3.2 and $3.9 \text{ m}^2_{\text{leaf}} \text{ m}^{-2}_{\text{soil}}$ during the first rotation. Additionally, Korkiakoski et al. (2023) estimated a five-year average GPP of $1406 \text{ gC m}^{-2} \text{ yr}^{-1}$ in a nutrient-rich peatland afforested with spruce and pine in the south of Finland, with an LAI slightly above 2 $\text{m}^2_{\text{leaf}} \text{ m}^{-2}_{\text{soil}}$ determined using remote sensing. Our GPP estimations for similar LAI values were around $1128 \text{ gC m}^{-2} \text{ yr}^{-1}$. Moreover, simulated GPP values during the first two years after clear-cutting (221 and $241 \text{ gC m}^{-2} \text{ yr}^{-1}$) closely align with those reported by Korkiakoski et al. (2019) for a nutrient-rich drained peatland post-clear-cut (175 and $298 \text{ gC m}^{-2} \text{ yr}^{-1}$).

4.2 On model limitations.

The model demonstrates a capability to reproduce GWL and soil temperature observations with reasonable accuracy. However, it simulates lower GWL during winter, likely due to its omission of the effects of freezing on water flow. Additionally, the underestimation of GWL during the driest summer periods may be attributed to inaccuracies in simulating. Evaporation and transpiration, which are influenced by root distribution and plant water use efficiency—parameters that were not calibrated. The model's simplistic approach to simulating drainage may also fail to capture critical hydrological dynamics, such as



465 anisotropic hydraulic conductivity, ditch geometry, or water-induced soil volume changes. Regarding temperature, the model tends to overestimate spring and summer temperatures. This overestimation may result from lower GWL at the onset of spring compared to observations, which reduces heat capacity and possibly heat conductivity. Furthermore, the simplistic upper boundary condition of the model, along with the lack of accounting for heat fluxes associated with soil surface evapotranspiration and the temperature modulation by trees, contributes to this discrepancy.

470 Despite these simplifications, the model provides a reasonable abiotic context for assessing carbon dynamics. It is essential, however, to evaluate the limitations on carbon representation on the model formulation and its implications in the results from this study. The model followed commonly used formulations for peat soils (Kleinen et al., 2012; Qiu et al., 2018), where peat is defined as a conceptual compartment with unspecified chemistry, that decomposes linearly according to a rate constants modified by environmental conditions. Limitations within this representation might explain why daily NEP fluxes were not

475 well represented by the model. Firstly, in current model structure, optimum moisture conditions for decomposition increase slowly with moisture content until field capacity, however the response might be faster in peat soils (Rewcastle et al., 2020; Ľupek et al., 2023). Furthermore, the complex redox chain that controls decomposition in peat soils is simplified by a function that only considers water content. In reality, non-saturated conditions can lead to limited aerobic conditions if strong decomposition depletes oxygen (Fan et al., 2014). Conversely, fully saturated conditions might not result in methane formation

480 if electron acceptors like nitrate or sulphate are available (Reddy & DeLaune, 2008).

The linear rate constants of decomposition are not adequate to capture non-linear responses such as respiration pulses at rewetting due to combined microbial reactivation and changes in substrate availability (Manzoni et al., 2020) or priming effects associated with substrate quality. It is well established that phenolic compounds can downregulate enzymes responsible for decomposing other carbon compounds, resulting in negative priming effects that inhibit overall decomposition (Freeman et

485 al., 2001). Conversely, allocation of labile carbon through roots can stimulate decomposer activity in coniferous-dominated soils (Jilková et al., 2022; Leppälampi-Kujansuu et al., 2014; Li et al., 2020). In nutrient-rich sites like the one simulated, this may be less significant than in nutrient-limited conditions, however the overall response of soil organic carbon decomposition to root exudates in coniferous forest remains unclear (Gundale et al., 2024). Interestingly, measurements of carbon sinks in soils from afforested drained peatlands often come from nutrient-poor sites and use methods that do not consider the effect of

490 labile carbon allocated by roots in heterotrophic respiration (Hermans et al., 2022).

The allocation of carbon within plant compartments follows a simplistic scheme where the allocation to root tissue is not directly influenced by water and nutrient availability. It is well-recognized that the proportion of carbon allocated to roots can increase when plants need to enhance their resource acquisition (Prescott et al., 2020). Additionally, the model maximizes foliage growth based on light conditions, but wood growth does not affect light availability. The way wood is represented in

495 the model implies some limitations. During the later stages of a forest rotation, when stand biomass is substantial, the model predicts that woody litter is the main form of carbon input to the soil. Additionally, wood respiration is identified as a primary source of CO₂. The current model version does not differentiate between sapwood and hardwood and assumes that wood turnover is proportional to wood biomass. In reality, growth is represented by new sapwood, which is the fraction that respire,



while sapwood gradually transforms into hardwood, and only a small portion of the bark ends up in the soil (Ogle & Pacala, 2009; Ukonmaanaho et al., 2008). The model could be improved with a more dynamic representation of wood dynamics. However, the allocation rates and respiration costs of sapwood are not well understood and are difficult to measure, posing challenges for accurately parameterizing a model given their importance in tree carbon dynamics (Metzler et al., 2024). Furthermore, the current model formulation implies a very strong response to elevated atmospheric CO₂ values that lead to very high photosynthetic rate during the second rotation causing twice the growth compared to the first rotation. This might be an overestimation based on values derived from CO₂ enrichment experiments (Bader et al., 2016; Uddling & Wallin, 2012). However, is still useful to analyse the system under very high carbon uptake values during the second rotation. Currently the model does not account for understory vegetation, in nutrient-rich afforested peatlands, grasses and mosses can dominate photosynthetic activity during the first 10 years of forest rotation (He et al., 2016). This exclusion may result in the model underestimating GPP and litter inputs during early years. Nonetheless, as evidenced by the measured data in this study, drained conditions during the initial years of forest rotation are likely characterized by significant carbon losses due to elevated decomposition of soil organic matter, especially when coupled with DNM (Korkiakoski et al., 2019; Palviainen et al., 2022). Furthermore, GHG emissions from ditches are also sensitive to DNM (Evans et al., 2016; Nieminen et al., 2018). Lastly, we assumed that a constant fraction of wood is allocated to HWP compartments. Our assumption that 65% of harvested wood has been used in other studies (Kasimir et al., 2018), however this fraction varies based on wood quality (Jonsson et al., 2018; Profft et al., 2009).

4.3 On system boundaries and metrics of carbon exchange

Assessing the net carbon exchanges (and thus the potential effect on climate) in afforested peatlands is intrinsically dependent on the delineation of system boundaries and the chosen evaluation metrics. This study argues that the optimal system boundaries to assess long term carbon exchanges encompass all inflows as atmospheric CO₂ uptake and all outflows as CO₂ released into the atmosphere—referred to here as “ecosystem+HWP”. Within these boundaries, different metrics can offer divergent perspectives on climatic effects. Our analysis reveals that towards the end of rotations, the system accumulated more carbon than it released, resulting in a positive NCB. However, NCB fails to account for the temporal dynamics of carbon accumulation within the system (Sierra, 2024). A small, constant carbon gain over time can yield the same NCB as carbon dynamics characterized by substantial initial losses followed by substantial later gains within the analysis period. However, these scenarios may not have equivalent effects on climate.

The influence of carbon dioxide on climate change, manifested through alterations in the planetary energy balance, depends on both the atmospheric CO₂ concentration and the residence time of each CO₂ molecule in the atmosphere (Joos et al., 2013). Consequently, when a system exhibits substantial carbon losses throughout the analysis period, only compensated towards the end, the interval during which accumulated losses exceeded accumulated gains can be interpreted as a period of negative effect on the climate, despite an eventual positive effect (i.e., accumulated losses became less than accumulated gains). Furthermore,



designating the end of the rotation as the final point of the analysis period introduces bias, as any accumulated carbon in biomass is relatively quickly lost upon harvesting.

This temporal information is captured by ICS, providing a more comprehensive assessment of the climatic impact of specific carbon dynamics within a system. This is especially important in drained peatlands where high carbon losses in the beginning
535 are compensated only towards the end of the rotation, leading to negative ICS. A substantial proportion of Fennoscandian drained afforested peatlands are approaching stand maturity, prompting imminent management decisions (Lehtonen et al., 2023). A very negative but improving ICS might be a representative pattern for these systems. It is thus important to assess the effect of different management strategies given this legacy effect on climate. Continuous forest cover (CCF) has been proposed as an alternative to manage current drained afforested peatlands (Laudon & Maher Hasselquist, 2023).

540 However, a limitation of the ICS is that it only considers carbon fluxes. N₂O fluxes are substantial in nutrient rich drained peatlands, and considering CH₄ emissions is necessary to assess rewetting as a management strategy (Jauhiainen et al., 2023; Kasimir et al., 2018). A metric that integrates all GHG through time considering the legacy effect of drainage is necessary to assess the management options to improve effects on climate from afforested drained peatlands. Given the relatively fast release of carbon from HWP after harvesting and potentially high release of potent CH₄ during initial years of successful
545 rewetting (Escobar et al., 2022), the effect on climate of combining clear cut and rewetting could take long to be compensated (Ojanen & Minkkinen, 2020).

5 Conclusions

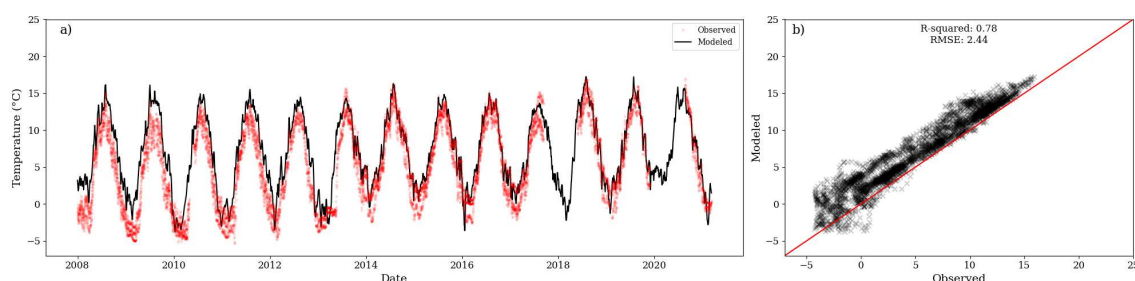
The ForSAFE-peat model was able to realistically reproduce soil abiotic (temperature and GWL) conditions at the drained and forested, nutrient rich peatland at Skogaryd. However, while the model could capture the observed net ecosystem exchange
550 reliably, it was unable to reproduce the daily observations of carbon exchange. The model predicted a substantial increase in biomass growth in the future following higher temperatures and atmospheric CO₂, supported by higher precipitation and nitrogen mineralisation, and shows that even such a large increase in photosynthesis may not compensate for the large carbon losses caused by draining peat soil. The results underline the importance of the choice of the system boundary considered in carbon budget estimates, and argues for a more holistic budget accounting for the ecosystem and the fate of the harvested
555 biomass. The study also shows how accounting for the temporal dimension of the carbon budget of a managed forest site can give fundamentally different estimates of the potential effect on climate warming. The study contrasts the NCB, which only focuses on book-keeping balances over a given period, with the more integrative ICS which accounts for the time CO₂ resides in the atmosphere, and indicates that the former may give misleading estimates of climatic implications. Based on the testing at Skogaryd, we show that even if the nutrient rich site may appear as a net sink at the end of a forest rotation, its legacy effect
560 on the climate can remain negative given that much of the captured carbon was released in the atmosphere longer than it was fixed at the site, thereby producing a warming effect. We finally argue for a pragmatic adoption of dynamic modelling in estimating the effects of forest management of climate warming despite their limitation as illustrated here, and underline the



importance of broader ecosystem boundaries in these estimates as well as more representative indicators accounting for the temporal aspect of forest management on carbon residence.

565 Appendix A: Further model performance evaluation.

Further evaluation of model was performed against temperature for depths of 0.15 m and 0.30 m. The modelled temperature at 0.20 m is similar to the observed temperature at 0.15m. However, slight overestimations are persistent (Figure A1).



570 **Figure A1. (a) Modelled temperature for the second layer (black line) and observations at 0.15m depth (red dots). (b) Correlation between observed and modelled values. During the period of comparison, the centroid of the first layer was between 0.215m and 0.22m**

Equally, the modelled temperature for a depth of 0.38m was similar the observed temperature at 0.30m (Figure A2).

575

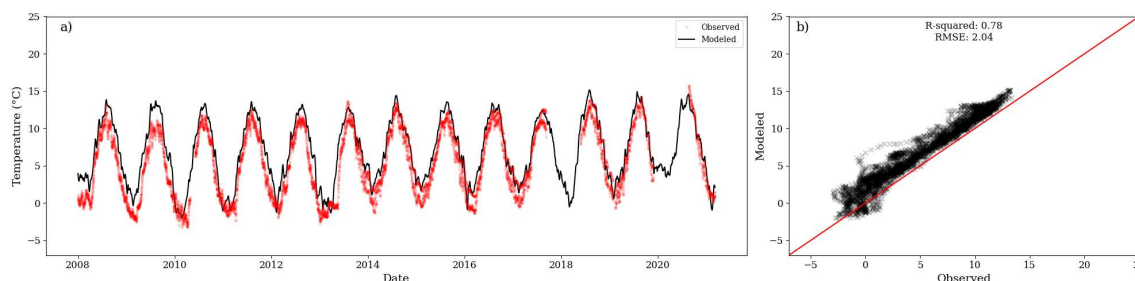
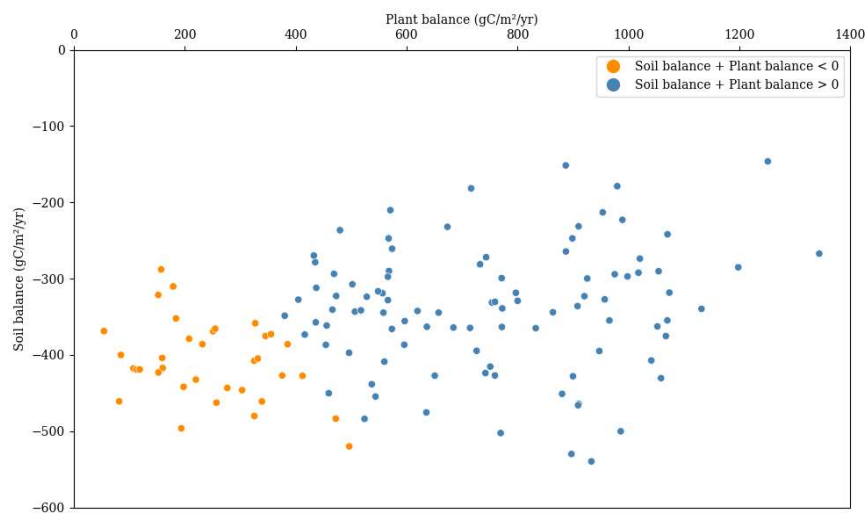


Figure A2. (a) Modelled temperature for the third layer (black line) and observations at 0.30m depth (red dots). (b) Correlation between observed and modelled values. During the period of comparison, the centroid of the first layer was between 0.39m and 0.38m



580 Appendix B: Carbon dynamics

The net plant carbon balance, expressed as the net primary productivity minus litterfall, is usually higher than the soil carbon losses and actively compensate for peat decomposition in normal years Figure B1. This explains the negative effect generated by harvesting.



585 **Figure B1. Relation between net primary productivity and soil balance. In orange values when the net between soil balance and NPP is negative and blue values when is positive.**

Code availability:

The original model code of ForSAFE-Peat is written in Fortran 90 and is freely available upon request to the model developers (see contact details above) with the intent to support new user in the initial stage of their work with the ForSAFE model.

590 Data availability:

Field measurement data used to validate the model, along with yearly model outputs of carbon fluxes encompassing the full extent of the simulation, are publicly available at [10.5281/zenodo.13626716](https://zenodo.org/record/13626716)

Author contribution:

DE led the study. DE, SB and SM conceptualized the study. DE and SB conducted the formal analysis and investigation. SM and JT assisted in the formal analysis and investigation. All the authors discussed the results together. DE wrote the original



draft of the paper and produced the figures, with feedback from SB and SM. All authors reviewed and commented on the original draft of the paper and its revisions.

Competing interest:

The authors declare that they have no conflict of interest

600 References

- Aber, J. D., Ollinger, S. V., & Driscoll, C. T. (1997). Modeling nitrogen saturation in forest ecosystems in response to land use and atmospheric deposition. *Ecological Modelling*, *101*(1), 61–78. [https://doi.org/10.1016/S0304-3800\(97\)01953-4](https://doi.org/10.1016/S0304-3800(97)01953-4)
- Aber, J. D., Reich, P. B., & Goulden, M. L. (1996). Extrapolating leaf CO₂ exchange to the canopy: A generalized model of forest photosynthesis compared with measurements by eddy correlation. *Oecologia*, *106*(2), 257–265. <https://doi.org/10.1007/BF00328606>
- 605
- Arnold, K. V., Weslien, P., Nilsson, M., Svensson, B. H., & Klemedtsson, L. (2005). Fluxes of CO₂, CH₄ and N₂O from drained coniferous forests on organic soils. *Forest Ecology and Management*, *210*(1), 239–254. <https://doi.org/10.1016/j.foreco.2005.02.031>
- 610 Bader, M. K.-F., Mildner, M., Baumann, C., Leuzinger, S., & Körner, C. (2016). Photosynthetic enhancement and diurnal stem and soil carbon fluxes in a mature Norway spruce stand under elevated CO₂. *Environmental and Experimental Botany*, *124*, 110–119. <https://doi.org/10.1016/j.envexpbot.2015.12.005>
- Bārdule, A., Petaja, G., Butlers, A., Purviņa, D., & Lazdiņš, A. (2021). Estimation of litter input in hemiboreal forests with drained organic soils for improvement of GHG inventories. *Baltic Forestry*, *27*(2), Article 2. <https://doi.org/10.46490/BF534>
- 615
- Blaško, R., Forsmark, B., Gundale, M. J., Lim, H., Lundmark, T., & Nordin, A. (2022). The carbon sequestration response of aboveground biomass and soils to nutrient enrichment in boreal forests depends on baseline site productivity. *Science of The Total Environment*, *838*, 156327. <https://doi.org/10.1016/j.scitotenv.2022.156327>



- Butlers, A., Laiho, R., Soosaar, K., Jauhiainen, J., Schindler, T., Bårdale, A., Kamil-Sardar, M., Haberl, A., Samariks, V.,
620 Vahter, H., Lazdiņš, A., Čiuldienė, D., Armolaitis, K., & Līcīte, I. (2024). Soil and forest floor carbon balance in
drained and undrained hemiboreal peatland forests. *EGUsphere*, 1–21. <https://doi.org/10.5194/egusphere-2024-1397>
- Crusius, J. (2020). “Natural” Climate Solutions Could Speed Up Mitigation, With Risks. Additional Options Are Needed.
Earths Future, 8(4), UNSP e2019EF001310. <https://doi.org/10.1029/2019EF001310>
- Darusman, T., Murdiyarso, D., Impron, & Anas, I. (2023). Effect of rewetting degraded peatlands on carbon fluxes: A meta-
625 analysis. *Mitigation and Adaptation Strategies for Global Change*, 28(3), 10. <https://doi.org/10.1007/s11027-023-10046-9>
- Engardt, M., & Langner, J. (2013). Simulations of future sulphur and nitrogen deposition over Europe using meteorological
data from three regional climate projections. *Tellus. Series B, Chemical and Physical Meteorology*, 65.
<https://urn.kb.se/resolve?urn=urn:nbn:se:smhi:diva-419>
- 630 Eriksson, S. (2021). *En laboratoriestudie om kol-, kväve- och fosforcykeln: Med fokus på kväveminalisation*.
INSTITUTIONEN FÖR BIOLOGI OCH MILJÖVETENSKAP.
- Ernfors, M., Rütting, T., & Klemmedtsson, L. (2011). Increased nitrous oxide emissions from a drained organic forest soil after
exclusion of ectomycorrhizal mycelia. *Plant and Soil*, 343(1), 161–170. <https://doi.org/10.1007/s11104-010-0667-9>
- Escobar, D., Belyazid, S., & Manzoni, S. (2022). Back to the Future: Restoring Northern Drained Forested Peatlands for
635 Climate Change Mitigation. *Frontiers in Environmental Science*, 10.
<https://www.frontiersin.org/article/10.3389/fenvs.2022.834371>
- Evans, C. D., Peacock, M., Baird, A. J., Artz, R. R. E., Burden, A., Callaghan, N., Chapman, P. J., Cooper, H. M., Coyle, M.,
Craig, E., Cumming, A., Dixon, S., Gauci, V., Grayson, R. P., Helfter, C., Heppell, C. M., Holden, J., Jones, D. L.,
Kaduk, J., ... Morrison, R. (2021). Overriding water table control on managed peatland greenhouse gas emissions.
640 *Nature*, 593(7860), Article 7860. <https://doi.org/10.1038/s41586-021-03523-1>
- Evans, C. D., Renou-Wilson, F., & Strack, M. (2016). The role of waterborne carbon in the greenhouse gas balance of drained
and re-wetted peatlands. *Aquatic Sciences*, 78(3), 573–590. <https://doi.org/10.1007/s00027-015-0447-y>



- Fan, Z., Neff, J. C., Waldrop, M. P., Ballantyne, A. P., & Turetsky, M. R. (2014). Transport of oxygen in soil pore-water systems: Implications for modeling emissions of carbon dioxide and methane from peatlands. *Biogeochemistry*, 645 121(3), 455–470. <https://doi.org/10.1007/s10533-014-0012-0>
- Guenther, A., Barthelmes, A., Huth, V., Joosten, H., Jurasinski, G., Koebisch, F., & Couwenberg, J. (2020). Prompt rewetting of drained peatlands reduces climate warming despite methane emissions. *Nature Communications*, 11(1), 1644. <https://doi.org/10.1038/s41467-020-15499-z>
- Gundale, M. J., Axelsson, E. P., Buness, V., Callebaut, T., DeLuca, T. H., Hupperts, S. F., Ibáñez, T. S., Metcalfe, D. B., 650 Nilsson, M.-C., Peichl, M., Spitzer, C. M., Stangl, Z. R., Strengbom, J., Sundqvist, M. K., Wardle, D. A., & Lindahl, B. D. (2024). The biological controls of soil carbon accumulation following wildfire and harvest in boreal forests: A review. *Global Change Biology*, 30(5), e17276. <https://doi.org/10.1111/gcb.17276>
- Haapalehto, T., Kotiaho, J. S., Matilainen, R., & Tahvanainen, T. (2014). The effects of long-term drainage and subsequent restoration on water table level and pore water chemistry in boreal peatlands. *Journal of Hydrology*, 519, 1493–1505. 655 <https://doi.org/10.1016/j.jhydrol.2014.09.013>
- He, H., Jansson, P.-E., Svensson, M., Björklund, J., Tarvainen, L., Klemmedtsson, L., & Kasimir, Å. (2016). Forests on drained agricultural peatland are potentially large sources of greenhouse gases – insights from a full rotation period simulation. *Biogeosciences*, 13(8), 2305–2318. <https://doi.org/10.5194/bg-13-2305-2016>
- Hermans, R., McKenzie, R., Andersen, R., Teh, Y. A., Cowie, N., & Subke, J.-A. (2022). Net soil carbon balance in afforested 660 peatlands and separating autotrophic and heterotrophic soil CO₂ effluxes. *Biogeosciences*, 19(2), 313–327. <https://doi.org/10.5194/bg-19-313-2022>
- Hilli, S. (2013). *Significance of litter production of forest stands and ground vegetation in the formation of organic matter and storage of carbon in boreal coniferous forests*. <https://jukuri.luke.fi/handle/10024/554803>
- Jauhiainen, J., Heikkinen, J., Clarke, N., He, H., Dalsgaard, L., Minkkinen, K., Ojanen, P., Vesterdal, L., Alm, J., Butlers, A., 665 Callesen, I., Jordan, S., Lohila, A., Mander, Ü., Óskarsson, H., Sigurdsson, B. D., Søgaard, G., Soosaar, K., Kasimir, Å., ... Laiho, R. (2023). Reviews and syntheses: Greenhouse gas emissions from drained organic forest soils –



synthesizing data for site-specific emission factors for boreal and cool temperate regions. *Biogeosciences*, 20(23), 4819–4839. <https://doi.org/10.5194/bg-20-4819-2023>

670 Jílková, V., Jandová, K., Cajthaml, T., Kukla, J., & Jansa, J. (2022). Differences in the flow of spruce-derived needle leachates and root exudates through a temperate coniferous forest mineral topsoil. *Geoderma*, 405, 115441. <https://doi.org/10.1016/j.geoderma.2021.115441>

Jonsson, R., Blujdea, V. N. B., Fiorese, G., Pilli, R., Rinaldi, F., Baranzelli, C., & Camia, A. (2018). Outlook of the European forest-based sector: Forest growth, harvest demand, wood-product markets, and forest carbon dynamics implications. *iForest - Biogeosciences and Forestry*, 11(2), 315. <https://doi.org/10.3832/ifer2636-011>

675 Joos, F., Roth, R., Fuglestedt, J. S., Peters, G. P., Enting, I. G., von Bloh, W., Brovkin, V., Burke, E. J., Eby, M., Edwards, N. R., Friedrich, T., Frölicher, T. L., Halloran, P. R., Holden, P. B., Jones, C., Kleinen, T., Mackenzie, F. T., Matsumoto, K., Meinshausen, M., ... Weaver, A. J. (2013). Carbon dioxide and climate impulse response functions for the computation of greenhouse gas metrics: A multi-model analysis. *Atmospheric Chemistry and Physics*, 13(5), 2793–2825. <https://doi.org/10.5194/acp-13-2793-2013>

680 Jovani-Sancho, A. J., Cummins, T., & Byrne, K. A. (2021). Soil carbon balance of afforested peatlands in the maritime temperate climatic zone. *Global Change Biology*, 27(15), 3681–3698. <https://doi.org/10.1111/gcb.15654>

Kasimir, Å., He, H., Coria, J., & Nordén, A. (2018). Land use of drained peatlands: Greenhouse gas fluxes, plant production, and economics. *Global Change Biology*, 24(8), 3302–3316. <https://doi.org/10.1111/gcb.13931>

685 Kleinen, T., Brovkin, V., & Schuldt, R. J. (2012). A dynamic model of wetland extent and peat accumulation: Results for the Holocene. *Biogeosciences*, 9(1), 235–248. <https://doi.org/10.5194/bg-9-235-2012>

Klemedtsson, L., Ernfors, M., Björk, R. G., Weslien, P., Rütting, T., Crill, P., & Sikström, U. (2010). Reduction of greenhouse gas emissions by wood ash application to a *Picea abies* (L.) Karst. Forest on a drained organic soil. *European Journal of Soil Science*, 61(5), 734–744. <https://doi.org/10.1111/j.1365-2389.2010.01279.x>

690 Korkiakoski, M., Ojanen, P., Tuovinen, J.-P., Minkkinen, K., Nevalainen, O., Penttilä, T., Aurela, M., Laurila, T., & Lohila, A. (2023). Partial cutting of a boreal nutrient-rich peatland forest causes radically less short-term on-site CO₂



emissions than clear-cutting. *Agricultural and Forest Meteorology*, 332, 109361.

<https://doi.org/10.1016/j.agrformet.2023.109361>

Korkiakoski, M., Tuovinen, J.-P., Penttilä, T., Sarkkola, S., Ojanen, P., Minkkinen, K., Rainne, J., Laurila, T., & Lohila, A. (2019). Greenhouse gas and energy fluxes in a boreal peatland forest after clear-cutting. *Biogeosciences*, 16(19),

695 3703–3723. <https://doi.org/10.5194/bg-16-3703-2019>

Krause, A., Knoke, T., & Rammig, A. (2020). A regional assessment of land-based carbon mitigation potentials: Bioenergy, BECCS, reforestation, and forest management. *Global Change Biology Bioenergy*, 12(5), 346–360.

<https://doi.org/10.1111/gcbb.12675>

Kreyling, J., Tanneberger, F., Jansen, F., van der Linden, S., Aggenbach, C., Blüml, V., Couwenberg, J., Emsens, W.-J.,

700 Joosten, H., Klimkowska, A., Kotowski, W., Kozub, L., Lennartz, B., Liczner, Y., Liu, H., Michaelis, D., Oehmke, C., Parakenings, K., Pleyl, E., ... Jurasinski, G. (2021). Rewetting does not return drained fen peatlands to their old selves. *Nature Communications*, 12(1), 5693. <https://doi.org/10.1038/s41467-021-25619-y>

Laudon, H., & Maher Hasselquist, E. (2023). Applying continuous-cover forestry on drained boreal peatlands; water regulation, biodiversity, climate benefits and remaining uncertainties. *Trees, Forests and People*, 11, 100363.

705 <https://doi.org/10.1016/j.tfp.2022.100363>

Lazdiņš, A., Lupiķis, A., Polmanis, K., Bārdule, A., Butlers, A., & Kalēja, S. (2024). Carbon stock changes of drained nutrient-rich organic forest soils in Latvia. *Silva Fennica*, 58(1). <https://www.silvafennica.fi/article/22017>

Lehtonen, A., Eyvindson, K., Härkönen, K., Leppä, K., Salmivaara, A., Peltoniemi, M., Salminen, O., Sarkkola, S., Launiainen, S., Ojanen, P., Rätty, M., & Mäkipää, R. (2023). Potential of continuous cover forestry on drained

710 peatlands to increase the carbon sink in Finland. *Scientific Reports*, 13(1), 15510. <https://doi.org/10.1038/s41598-023-42315-7>

Leifeld, J., Wüst-Galley, C., & Page, S. (2019). Intact and managed peatland soils as a source and sink of GHGs from 1850 to 2100. *Nature Climate Change*, 9(12), 945–947. <https://doi.org/10.1038/s41558-019-0615-5>



- 715 Leppä, K., Hökkä, H., Laiho, R., Launiainen, S., Lehtonen, A., Mäkipää, R., Peltoniemi, M., Saarinen, M., Sarkkola, S., & Nieminen, M. (2020). Selection Cuttings as a Tool to Control Water Table Level in Boreal Drained Peatland Forests. *Frontiers in Earth Science*, 8. <https://doi.org/10.3389/feart.2020.576510>
- Leppälampi-Kujansuu, J., Salemaa, M., Kleja, D. B., Linder, S., & Helmisaari, H.-S. (2014). Fine root turnover and litter production of Norway spruce in a long-term temperature and nutrient manipulation experiment. *Plant and Soil*, 374(1), 73–88. <https://doi.org/10.1007/s11104-013-1853-3>
- 720 Li, J., Zhou, M., Alaei, S., & Bengtson, P. (2020). Rhizosphere priming effects differ between Norway spruce (*Picea abies*) and Scots pine seedlings cultivated under two levels of light intensity. *Soil Biology and Biochemistry*, 145, 107788. <https://doi.org/10.1016/j.soilbio.2020.107788>
- Liu, H., Price, J., Rezanezhad, F., & Lennartz, B. (2020). Centennial-Scale Shifts in Hydrophysical Properties of Peat Induced by Drainage. *Water Resources Research*, 56(10), e2020WR027538. <https://doi.org/10.1029/2020WR027538>
- 725 Maljanen, M., Shurpali, N., Hytönen, J., Mäkiranta, P., Aro, L., Potila, H., Laine, J., Li, C., & Martikainen, P. J. (2012). Afforestation does not necessarily reduce nitrous oxide emissions from managed boreal peat soils. *Biogeochemistry*, 108(1/3), 199–218. <https://www.jstor.org/stable/41410591>
- Manzoni, S., Čapek, P., Porada, P., Thurner, M., Winterdahl, M., Beer, C., Brüchert, V., Frouz, J., Herrmann, A. M., Lindahl, B. D., Lyon, S. W., Šantrůčková, H., Vico, G., & Way, D. (2018). Reviews and syntheses: Carbon use efficiency from organisms to ecosystems – definitions, theories, and empirical evidence. *Biogeosciences*, 15(19), 5929–5949. <https://doi.org/10.5194/bg-15-5929-2018>
- 730 Menberu, M. W., Tahvanainen, T., Marttila, H., Irannezhad, M., Ronkanen, A.-K., Penttinen, J., & Kløve, B. (2016). Water-table-dependent hydrological changes following peatland forestry drainage and restoration: Analysis of restoration success. *Water Resources Research*, 52(5), 3742–3760. <https://doi.org/10.1002/2015WR018578>
- 735 Metzler, H., Launiainen, S., & Vico, G. (2024). Amount of carbon fixed, transit time and fate of harvested wood products define the climate change mitigation potential of boreal forest management—A model analysis. *Ecological Modelling*, 491, 110694. <https://doi.org/10.1016/j.ecolmodel.2024.110694>



- Meyer, A., Tarvainen, L., Nousratpour, A., Björk, R. G., Ernfors, M., Grelle, A., Kasimir Klemetsson, Å., Lindroth, A., Rantfors, M., Rütting, T., Wallin, G., Weslien, P., & Klemetsson, L. (2013). A fertile peatland forest does not
740 constitute a major greenhouse gas sink. *Biogeosciences*, *10*(11), 7739–7758. <https://doi.org/10.5194/bg-10-7739-2013>
- Minkinen, K., Laine, J., Shurpali, N. J., Mäkiranta, P., Alm, J., & Penttilä, T. (2007). *Heterotrophic soil respiration in forestry-drained peatlands*. <https://jukuri.luke.fi/handle/10024/513693>
- Minkinen, K., Ojanen, P., Koskinen, M., & Penttilä, T. (2020). Nitrous oxide emissions of undrained, forestry-drained, and
745 rewetted boreal peatlands. *Forest Ecology and Management*, *478*, 118494. <https://doi.org/10.1016/j.foreco.2020.118494>
- Minkinen, K., Ojanen, P., Penttilä, T., Aurela, M., Laurila, T., Tuovinen, J.-P., & Lohila, A. (2018). Persistent carbon sink at a boreal drained bog forest. *BIOGEOSCIENCES*, *15*(11), 3603–3624. <https://doi.org/10.5194/bg-15-3603-2018>
- Munthe, J., Arnell, J., Moldan, F., Karlsson, P. E., Åström, S., Gustafsson, T., Kindbom, K., Hellsten, S., Hansen, K.,
750 Jutterström, S., Lindblad, M., Tekie, H., Malmaeus, M., & Kronnäs, V. (2016). *Klimatförändringen och miljömål*. IVL Svenska Miljöinstitutet. <https://urn.kb.se/resolve?urn=urn:nbn:se:ivl:diva-356>
- Nieminen, M., Piirainen, S., Sikström, U., Löfgren, S., Marttila, H., Sarkkola, S., Laurén, A., & Finér, L. (2018). Ditch network maintenance in peat-dominated boreal forests: Review and analysis of water quality management options. *Ambio*, *47*(5), 535–545. <https://doi.org/10.1007/s13280-018-1047-6>
- 755 Noebel, R. (2023). *WHY IS PEATLAND REWETTING CRITICAL FOR MEETING EU ENVIRONMENTAL OBJECTIVES?* IEEP.
- Nyström, E. (2016). *The Geology of the Skogaryd Research Catchment, Sweden: A Basis for Future Hydrogeological Research*. Department of Earth Sciences, University of Gothenburg.
- Ogle, K., & Pacala, S. W. (2009). A modeling framework for inferring tree growth and allocation from physiological,
760 morphological and allometric traits. *Tree Physiology*, *29*(4), 587–605. <https://doi.org/10.1093/treephys/tpn051>
- Ojanen, P., & Minkinen, K. (2019). The dependence of net soil CO₂ emissions on water table depth in boreal peatlands drained for forestry. *MIRES AND PEAT*, *24*, 27. <https://doi.org/10.19189/MaP.2019.OMB.StA.1751>



- Ojanen, P., & Minkkinen, K. (2020). Rewetting Offers Rapid Climate Benefits for Tropical and Agricultural Peatlands But Not for Forestry-Drained Peatlands. *Global Biogeochemical Cycles*, 34(7), e2019GB006503.
765 <https://doi.org/10.1029/2019GB006503>
- Ojanen, P., Minkkinen, K., Alm, J., & Penttilä, T. (2010). Soil–atmosphere CO₂, CH₄ and N₂O fluxes in boreal forestry-drained peatlands. *Forest Ecology and Management*, 260(3), 411–421. <https://doi.org/10.1016/j.foreco.2010.04.036>
- Palviainen, M., Peltomaa, E., Laurén, A., Kinnunen, N., Ojala, A., Berninger, F., Zhu, X., & Pumpanen, J. (2022). Water quality and the biodegradability of dissolved organic carbon in drained boreal peatland under different forest
770 harvesting intensities. *Science of The Total Environment*, 806, 150919.
<https://doi.org/10.1016/j.scitotenv.2021.150919>
- Prescott, C. E., Grayston, S. J., Helmisaari, H.-S., Kaštovská, E., Körner, C., Lambers, H., Meier, I. C., Millard, P., & Ostonen, I. (2020). Surplus Carbon Drives Allocation and Plant–Soil Interactions. *Trends in Ecology & Evolution*, 35(12), 1110–1118. <https://doi.org/10.1016/j.tree.2020.08.007>
- 775 Profft, I., Mund, M., Weber, G.-E., Weller, E., & Schulze, E.-D. (2009). Forest management and carbon sequestration in wood products. *European Journal of Forest Research*, 128(4), 399–413. <https://doi.org/10.1007/s10342-009-0283-5>
- Qiu, C., Zhu, D., Ciais, P., Guenet, B., Krinner, G., Peng, S., Aurela, M., Bernhofer, C., Brümmer, C., Bret-Harte, S., Chu, H., Chen, J., Desai, A. R., Dušek, J., Euskirchen, E. S., Fortuniak, K., Flanagan, L. B., Friborg, T., Grygoruk, M., ... Ziemblinska, K. (2018). ORCHIDEE-PEAT (revision 4596), a model for northern peatland CO₂, water, and energy
780 fluxes on daily to annual scales. *Geoscientific Model Development*, 11(2), 497–519. <https://doi.org/10.5194/gmd-11-497-2018>
- Ranniku, R., Mander, Ü., Escuer-Gatius, J., Schindler, T., Kupper, P., Sellin, A., & Soosaar, K. (2024). Dry and wet periods determine stem and soil greenhouse gas fluxes in a northern drained peatland forest. *Science of The Total Environment*, 928, 172452. <https://doi.org/10.1016/j.scitotenv.2024.172452>
- 785 Reddy, K. R., & DeLaune, R. D. (2008). Carbon. In *Biogeochemistry of Wetlands*. CRC Press.



- Rewcastle, K. E., Moore, J. A. M., Henning, J. A., Mayes, M. A., Patterson, C. M., Wang, G., Metcalfe, D. B., & Classen, A. T. (2020). Investigating drivers of microbial activity and respiration in a forested bog. *Pedosphere*, 30(1), 135–145. [https://doi.org/10.1016/S1002-0160\(19\)60841-6](https://doi.org/10.1016/S1002-0160(19)60841-6)
- 790 Rogelj, J., Shindell, D., Jiang, K., Fifita, S., Forster, P., Ginzburg, V., Handa, C., Kobayashi, S., Kriegler, E., Mundaca, L., Séférian, R., Vilariño, M. V., Calvin, K., Emmerling, J., Fuss, S., Gillett, N., He, C., Hertwich, E., Höglund-Isaksson, L., ... Schaeffer, R. (2018). *Mitigation Pathways Compatible with 1.5°C in the Context of Sustainable Development* (p. 82). IPCC.
- 795 Seddon, N., Chausson, A., Berry, P., Girardin, C. A. J., Smith, A., & Turner, B. (2020). Understanding the value and limits of nature-based solutions to climate change and other global challenges. *Philosophical Transactions of the Royal Society B-Biological Sciences*, 375(1794), 20190120. <https://doi.org/10.1098/rstb.2019.0120>
- Sierra, C. A. (2024). Integrating time in definitions of carbon sequestration and greenhouse gas removals and reversals. *In Review in Royal Society Open Science*.
- Sierra, C. A., Crow, S. E., Heimann, M., Metzler, H., & Schulze, E.-D. (2021). The climate benefit of carbon sequestration. *Biogeosciences*, 18(3), 1029–1048. <https://doi.org/10.5194/bg-18-1029-2021>
- 800 Tanneberger, F., Appulo, L., Ewert, S., Lakner, S., Ó Brolcháin, N., Peters, J., & Wichtmann, W. (2021). The Power of Nature-Based Solutions: How Peatlands Can Help Us to Achieve Key EU Sustainability Objectives. *Advanced Sustainable Systems*, 5(1), 2000146. <https://doi.org/10.1002/adsu.202000146>
- 805 Tong, C. H. M., Noumonvi, K. D., Ratcliffe, J., Laudon, H., Järveoja, J., Drott, A., Nilsson, M. B., & Peichl, M. (2024). A drained nutrient-poor peatland forest in boreal Sweden constitutes a net carbon sink after integrating terrestrial and aquatic fluxes. *Global Change Biology*, 30(3), e17246. <https://doi.org/10.1111/gcb.17246>
- Župek, B., Lehtonen, A., Yurova, A., Abramoff, R., Manzoni, S., Guenet, B., Bruni, E., Launiainen, S., Peltoniemi, M., Hashimoto, S., Tian, X., Heikkinen, J., Minkkinen, K., & Mäkipää, R. (2023). Modeling boreal forest's mineral soil and peat C stock dynamics with Yasso07 model coupled with updated moisture modifier. *EGUsphere*, 1–34. <https://doi.org/10.5194/egusphere-2023-1523>



- 810 Uddling, J., & Wallin, G. (2012). Interacting effects of elevated CO₂ and weather variability on photosynthesis of mature boreal Norway spruce agree with biochemical model predictions. *Tree Physiology*, *32*(12), 1509–1521. <https://doi.org/10.1093/treephys/tps086>
- Ukonmaanaho, L., Merilä, P., Nöjd, P., & Nieminen, T. M. (2008). *Litterfall production and nutrient return to the forest floor in Scots pine and Norway spruce stands in Finland*. <https://jukuri.luke.fi/handle/10024/514741>
- 815 Uri, V., Kukumagi, M., Aosaar, J., Varik, M., Becker, H., Morozov, G., & Karoles, K. (2017). Ecosystems carbon budgets of differently aged downy birch stands growing on well-drained peatlands. *Forest Ecology and Management*, *399*, 82–93. <https://doi.org/10.1016/j.foreco.2017.05.023>
- Vestin, P., Mölder, M., Kljun, N., Cai, Z., Hasan, A., Holst, J., Klemetsson, L., & Lindroth, A. (2020). Impacts of Clear-Cutting of a Boreal Forest on Carbon Dioxide, Methane and Nitrous Oxide Fluxes. *Forests*, *11*(9), Article 9.
- 820 <https://doi.org/10.3390/fl11090961>
- Wallman, P., Svensson, M. G. E., Sverdrup, H., & Belyazid, S. (2005). ForSAFE—an integrated process-oriented forest model for long-term sustainability assessments. *Forest Ecology and Management*, *207*(1), 19–36. <https://doi.org/10.1016/j.foreco.2004.10.016>
- Wilson, D., Blain, D., Couwenberg, J., Evans, C. D., Murdiyarso, D., Page, S. E., Renou-Wilson, F., Rieley, J. O., Sirin, A.,
- 825 Strack, M., & Tuittila, E.-S. (2016). Greenhouse gas emission factors associated with rewetting of organic soils. *Mires and Peat*, *17*. <https://doi.org/10.19189/MaP.2016.OMB.222>
- Yu, L., Zanchi, G., Akselsson, C., Wallander, H., & Belyazid, S. (2018). Modeling the forest phosphorus nutrition in a southwestern Swedish forest site. *Ecological Modelling*, *369*, 88–100. <https://doi.org/10.1016/j.ecolmodel.2017.12.018>
- 830 Zanchi, G., Lucander, K., Kronnäs, V., Lampa, M. E., & Akselsson, C. (2021a). Modelling the effects of forest management intensification on base cation concentrations in soil water and on tree growth in spruce forests in Sweden. *European Journal of Forest Research*, *140*(6), 1417–1429. <https://doi.org/10.1007/s10342-021-01408-6>



Zanchi, G., Yu, L., Akselsson, C., Bishop, K., Köhler, S., Olofsson, J., & Belyazid, S. (2021b). Simulation of water and chemical transport of chloride from the forest ecosystem to the stream. *Environmental Modelling & Software*, 138, 835–845. <https://doi.org/10.1016/j.envsoft.2021.104984>

840

845

850